SPATIAL DISTRIBUTION AND TEMPORAL VARIABILITY OF LITHOGENIC PARTICLES IN FIRST-YEAR SEA ICE AND CONDITIONS RESPONSIBLE FOR PARTICLE ENTRAINMENT

By

Aaron Patrick Stierle

RECOMMENDED:

Dr. Narayan Naidu

Susan A. Henrichs

Hajo Eicken

Advisory Committee Chair

Paul W. Layer

Department Head

APPROVED:

D. Woodall

Dean, College of Science, Engineering and Mathematics

M. R. Kan

Dean of the Graduate School

12-5-01

Date

SPATIAL DISTRIBUTION AND TEMPORAL VARIABILITY OF LITHOGENIC PARTICLES IN FIRST-YEAR SEA ICE AND CONDITIONS RESPONSIBLE FOR PARTICLE ENTRAINMENT

A

THESIS

Presented to the Faculty

of the University of Alaska Fairbanks

in Partial Fulfillment of the Requirements

for the Degree of

MASTER OF SCIENCE

By

Aaron Patrick Stierle, B.S.

Fairbanks, Alaska

December 2001

Abstract

Processes controlling the spatial and temporal variability of sea ice sediment inclusions in the shallow-marine environment of Elson Lagoon near Barrow, Alaska, were studied by modeling the potential for sediment resuspension during the 1998, 1999 and 2000 fall freeze-up events and examining sea ice cores from the post-freeze-up ice cover. Resuspension potential was controlled spatially by the local bathymetry and interannually by wind speed and fetch. Increases in resuspension potential corresponded to greater sea ice sediment content. Sediments occurred exclusively as aggregates confined to brine inclusions in the ice and exhibited a tendency toward a clustered spatial distribution, because of their exclusion from growing frazil ice crystals. Sea ice sediment concentrations ranged from 24 mg/l to 1474 mg/l and were positively correlated with the cross-sectional area of aggregates and negatively correlated with the minimum distance between neighboring aggregates, implying that sediment aggregation occurred during the solidification of the ice cover.

Table of Contents

List of Figures

List of Tables

Acknowledgments

Special thanks to my committee members, Hajo Eicken, Sathy Naidu and Susan Henrichs, for encouragement and enlightening discussions on topics related to my research. Funding for this project came from NSF (LExEn) Grant OPP-9817738. Dave Ramey and the Barrow Arctic Science Consortium provided exceptional logistical support in the field. Computational support was provided by the Arctic Region Supercomputing Center. Karen Junge, Christopher Krembs, Karoline Frey and Andy Mahoney offered assistance in the field, even if it meant missing lunch occasionally. Kevin Engle and Shari George were instrumental in sharpening my computer skills, particularly when dealing with TerraScan and ArcInfo. I especially want to thank my family for moral and financial support that allowed me to realize my dream of coming to the great state of Alaska.

Chapter 1

Introduction

Concerns over greenhouse gas-induced global warming have stimulated interest in evaluating the response of polar regions to anthropogenic changes in the earth system. Recent fluctuations in both the areal extent of Arctic sea ice and rates of coastal erosion around the Arctic Ocean suggest that this environment is changing (Are, 1998; Serreze et al., 2000). The harsh climate and remoteness hamper data acquisition in the Arctic as compared to temperate marine environments, making it difficult to attribute changes to anthropogenic and/or natural causes. Moreover, without a clear picture of the sources of natural variability in the Arctic environment, it is difficult to assess the importance of these sources in explaining changes in the Arctic.

1.1 Distribution of sediment in sea ice

Recent studies suggest that significant natural variability exists in the sediment content of Arctic sea ice (Figure 1; Reimnitz and Kempema, 1987; Clark, 1990; Nürnberg et al, 1994; Reimnitz et al., 1994). The presence of sediments in sea ice has been found to reduce the albedo of ice and increase the absorption of shortwave radiation by the ice cover (Light et al., 1998). Satellite observations show a distinct patchiness in the distribution of sediments in sea ice on the scale of kilometers, while shipboard observations reveal a similar pattern down to the centimeter-scale (Nürnberg et al., 1994; Eicken et al, 2000a). Nevertheless, these observations are spotty due to inclement weather and logistical costs and tend to undersample the spatial distribution of sedimentary inclusions.

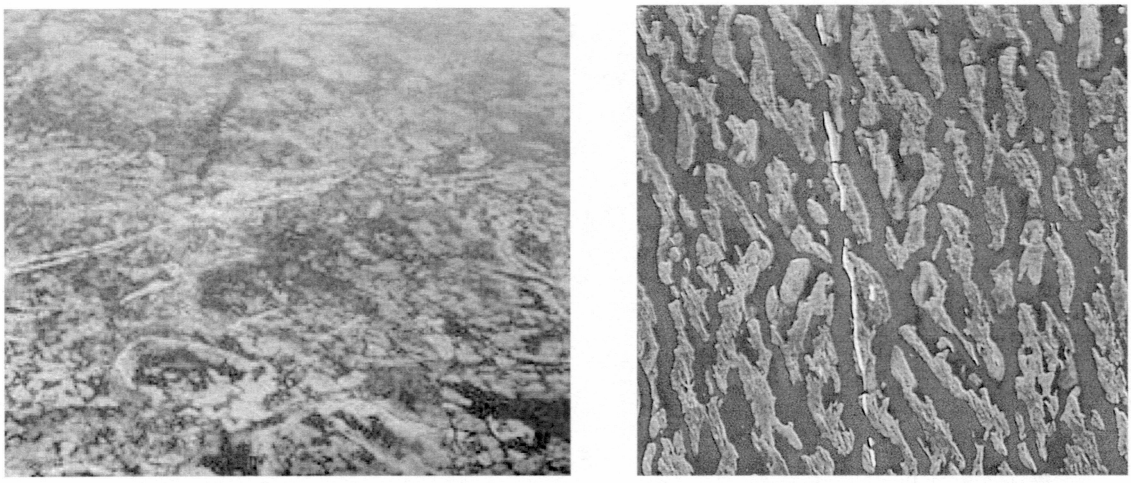

Figure 1. Patchy nature of sediment in sea ice. The two aerial photographs of sediment-laden sea illustrate the variability in the sediment content of sea ice. The left photo is from the Siberian Arctic and the right photo is from Elson Lagoon in 2000. In these photos, the darkest areas are melt ponds. Intermediate shades of gray represent sea ice with varying concentrations of sediment (darker gray = higher sediment concentration). In the left photo, clean and snow-covered ice appear white. The linear white features in the right photo represent subaerial exposures of clean sea ice that formed when the original sediment-laden ice cover fractured. The left photo is approximately 150 m wide and the right is approximately 150 m wide.

Undersampling occurs for two reasons. First, satellite observations examine only the upper 10 cm of the ice cover at most, as it is this portion of the sea ice cover that determines albedo. However, relatively high sediment concentrations are routinely observed deeper in the ice cover, especially in first-year sea ice (e.g., Osterkamp and Gosink, 1984, Eicken et al., 1997). Second, given the abundance of micrometer-sized particles (Nürnberg et al., 1994) and brine inclusions (Perovich and Gow, 1996), such observations are likely not representative of the micro- to millimeter-scale spatial distribution of sediments in sea ice. Yet, the sub-centimeter-scale spatial distribution of entrained sediments may significantly affect various processes both within and outside the sea ice cover. Thus, an approach that more accurately predicts the distribution of

sediments over a range of scales needs to be developed so that the role sedimentary inclusions play in processes operating in the sea ice environment can be better quantified.

1.2 Historical research on sediment entrainment

Observations of sediment-laden sea ice extending back at least four centuries have led to a number of hypotheses concerning the entrainment of sediments into sea ice. Prior to the 1950's, it was commonly believed that eolian deposition, riverine overflow, sea floor adfreezing and mass wasting events were the primary sources of the entrained sediments. However, both eolian deposition and riverine overflow have since been discounted as important entrainment mechanisms (Barnes and Reimnitz, 1974; Darby et al., 1974). Reimnitz et al. (1987) suggested that anchor ice could introduce substantial amounts of sediment into the sea ice cover, but its occurrence was too patchy to explain the large areas of sediment-laden ice observed in the Arctic Ocean. They noted that anchor ice formation was limited to regions with a coarse-grained or ice-bonded substrate. Another potential entrainment mechanism was suggested by Campbell and Collin (1958) that better fit their observations in Foxe Basin in the Canadian Archipelago. They hypothesized that sediments were frozen into sea ice when ice formation coincided with an increase in water turbidity due to the resuspension of bottom sediments through the action of waves, tides and currents. Campbell and Collin termed this process "suspension freezing". Sharma (1974) postulated a mechanism very similar to suspension freezing to explain the presence of sediment-laden sea ice in the eastern Bering Sea. From studies of lagoons along the Alaskan Beaufort Sea coast, Naidu et al. (1984) hypothesized that wave-induced resuspension of poorly-cohesive, fine-grained bottom sediments resulted in

increased turbidity in shallow areas and, when such events coincided with fall freeze-up, the entrainment of sediments into sea ice. To account for the apparent enrichment of sediments in sea ice versus ambient water column concentrations, Naidu et al. (1980) proposed a sediment concentrating mechanism whereby accreting frazil ice crystals drift through turbid seawater and trap sediments in the ice. Dethleff et al. (1998) concluded that a filtration mechanism consistent with Naidu et al.'s (1980) idea could be operating in surface grease ice streaks where convergent oceanic vortices circulate turbulent seawater through aggregated frazil ice crystals. In 1984, Osterkamp and Gosink reviewed the possible entrainment mechanisms and concluded that a combination of suspension freezing and sediment filtration was most likely the dominant mechanism of sediment entrainment into sea ice in the Arctic Ocean. Osterkamp and Gosink (1984) also presented evidence that entrained sediments are concentrated in brine inclusions (grain boundaries and the intersections of three or more grains (triple junctions)) and air bubbles. Furthermore, Osterkamp and Gosink hypothesized the downward migration of a freeze front during the solidification of the ice cover to explain the observed vertical distribution of entrained sediments. In 1989, Kempema et al. found that during stormy periods on the Beaufort Sea shelf, the concentration of suspended sediments could reach levels observed in sea ice, and suggested that there was no need to invoke a separate mechanism to concentrate sediments in sea ice. Most recently, a series of laboratory experiments led Zatsepin and Golovin (2001) to suggest that frazil ice formation at the interface between river water and seawater could introduce significant amounts of sediment into the ice cover.

Quantitative studies attempting to relate meteorology, wave climate and bottom sediment resuspension in Arctic waters were begun in the early 1970's. Sharma et al. (1972) working in the Bering Sea used meteorological data and wave forecast theory to estimate the oscillatory current velocity of near-bed water parcels and the size of sedimentary particles that could be entrained in the water column. Wiseman et al. (1973) found that current speeds were much greater during the summer open-water season than during the winter ice-covered season, but due to the failure of deployed current meters they were unable to quantify the relationship between wind speed and fetch and bottom sediment resuspension. In a study on coarse-grained sediment dynamics, Nummedal (1979) attempted to relate sediment transport to the energy of wave-generated longshore currents. He suggested that during the open water season along the north coast of Alaska, material coarser than fine sand moves only in response to wind-induced (littoral) currents, as tidal currents are weak in this region. Cacchione and Drake (1979) and Caccione et al. (1982) conducted experiments in Norton Sound, AK, to determine the frequency with which threshold conditions for sea floor sediment movement were exceeded. These experiments showed that even during maximum tidal current velocities (such as during spring tides) only limited bottom sediment resuspension occurred, while significant resuspension frequently occurred when oscillatory currents generated by wind-induced waves contributed to the bottom stress already exerted by tidal and permanent ocean currents. In a series of experiments between 1978 and 1982, Naidu et al. (1982) deployed an instrumented tripod in Simpson Lagoon, north Arctic Alaska. This tripod was equipped with a nephelometer to measure suspended sediment

concentrations, a pressure sensor for determining the wave climate and a current meter to measure current velocities. Naidu et al. (1982) encountered difficulties in obtaining reliable current speed measurements, but estimated that wind speeds in excess of 8.1 m/s were required to resuspend poorly cohesive bottom sediments in lagoons along the north coast of Alaska. Studies in the Canadian Beaufort Sea have revealed that sediment resuspension during storms is affected by the depth to which the effects of the storm are felt (Hill et al., 1991). It was found that oscillatory current motion occurs at greater depths under passing waves as the surface wind velocity increases. In addition, the current velocity at a given depth increases as the wind velocity increases. Hill et al (1991) estimated that fine-grained sediments could only be resuspended from depths greater than 10 m only once per year or less frequently in conjunction with the passage of particularly intense storms. It was also found that, in shallow areas prone to frequent resuspension, clay-size particles were selectively removed from bottom muddy sediments, leaving silt and altering the amount of shear stress required for sediment resuspension. More recently, Sherwood (2000) used a modeling approach to verify that fine-grained, poorly cohesive sea floor sediments could be entrained into sea ice that was forming in shallow, unstratified water made turbulent by strong, cold winds blowing over long fetches.

1.3 Sediment entrainment process

Although the processes by which sediment is entrained into the sea ice cover during suspension freezing are not completely understood, a hypothesis has grown out of the limited body of knowledge that relates meteorological conditions, wave climate, frazil ice

formation and sediment resuspension (Naidu et al, 1984; Reimnitz et al., 1993; Sherwood, 2000). Subfreezing air temperatures in conjunction with turbulent mixing of the water column by storm waves and thermohaline processes result in the formation of frazil ice over the entire depth of the ocean mixed layer. Simultaneously, turbulent shear at the ocean-seabed boundary over shallow shelves leads to resuspension of marine sediments. In turbulent environments, frazil ice crystals appear to remove suspended sediments from the water column either by collecting them on the surfaces of individual ice crystals or in the interstices of flocs of ice crystals. Once the turbulent mixing abates, buoyant frazil ice crystals rise to the sea surface, scavenging remaining suspended sedimentary particles from the water column. At any time, if an ice crystal becomes negatively buoyant due to an excess of attached sedimentary particles, the crystal will sink unless an environmental disturbance (turbulence, particle collision, wave, etc.) causes the excess particles to be dislodged. Continued subfreezing air temperatures cause ice formation in the interstices of the resulting slushy layer (congelation). During the congelation process, the sediment inclusions are speculated to be excluded from the ice crystal lattice and physically aggregated in the brine inclusions (Osterkamp and Gosink, 1984). Congelation experiments in the laboratory suggest that some sediment may also be redistributed in or lost from the frazil layer ahead of the freeze front (Clayton et al., 1990).

1.4 Sediment sources

Shallow shelf regions surrounding the deep basins of the Arctic Ocean may serve as a significant source of the sediment incorporated into the Arctic sea ice (Figure 2).

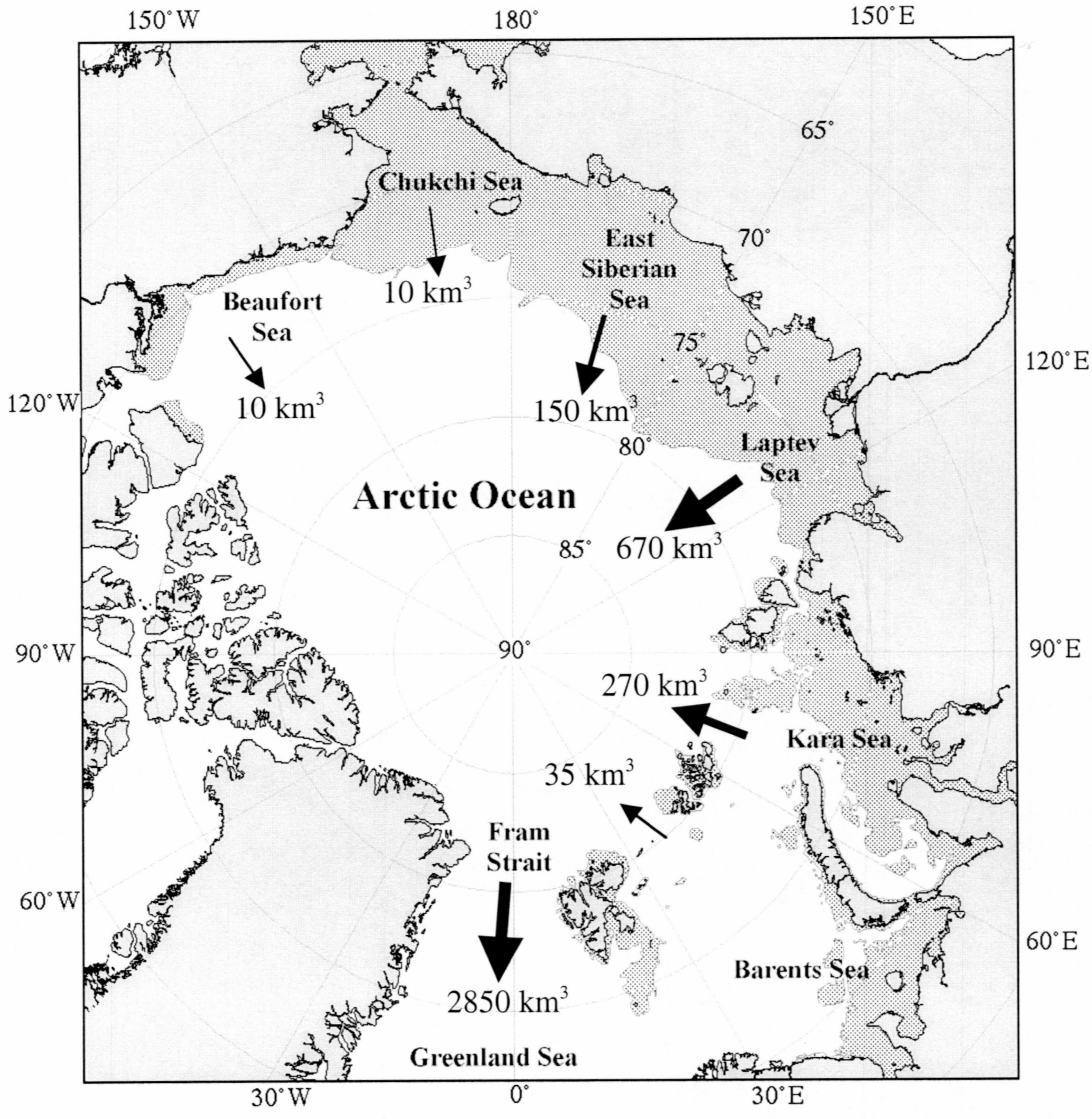

Figure 2. Continental shelf regions contributing sediments to Arctic sea ice. Stippled regions represent continental shelves that are less than 100 m deep. Landmasses are represented in gray. Arrows represent the volume of sea ice exported from each region. (H. Eicken, unpublished).

Provenance studies suggest that the shallow shelves of the Laptev and Kara Seas contribute most of the sediment seen in Arctic sea ice, although those of the East Siberian and Beaufort Seas appear to be minor source areas as well (Reimnitz et al., 1993; Pfirman et al., 1997; Eicken et al., 2000a). These shallow shelf regions, often lying within the zone of open water at the end of summer and beginning of the fall freeze-up season, are frequented by intense storms generated by the presence of low-pressure systems around there. Such storms provide favorable conditions for both sediment resuspension from the shallow sea floor and the formation of significant frazil and slush sea ice. Moreover, it appears that the interannual variability in location, timing and intensity of storms around freeze-up results in the discontinuous occurrence of sediment-laden ice across the Arctic Ocean (Nürnberg et al., 1994).

1.5 Textures of sediment-laden sea ice

Sediment-laden sea ice exhibits two different types of textures, which appear to be directly related to the entrainment mechanism involved (Barnes et al., 1982). In some samples sediments cover a large range of grain sizes and occur in patches in the ice, whereas sediments in other samples are predominantly fine grained and evenly distributed within the ice. The first type suggests entrainment by direct contact between ice and the sea floor (e.g., anchor ice and ice gouging). The second type suggests that suspension freezing and/or filtration were the dominant entrainment mechanism(s). Both anchor ice and suspension freezing form in a turbulent water column (Reimnitz et al., 1987). Additionally, anchor ice formation requires that either a coarse-grained (> fine sand) or ice-bonded substrate exists. Adherence of frazil ice to coarse-grained and ice-

bonded substrates overcomes the buoyancy and drag resistance of the ice, and thus allows it to remain in contact with the sea floor.

1.6 Effects of entrained sediments on sea ice properties

Once entrained, sediments affect the properties of the ice cover. Light et al. (1998) found that the albedo of sea ice is reduced when sediment is present in the ice cover and that the magnitude of this decrease is dependent on the size of sediment inclusions (among other factors), which may differ from the particle size of the entrained material. The reduced albedo of sediment-laden sea ice is thought to enhance summer melting and could potentially decrease the areal extent of the ice cover (Ledley and Pfirman, 1997). A decrease in the areal extent of the ice cover could threaten polar ecosystems by way of habitat loss (Tynan and DeMaster, 1997) and alter global climate through an increase in the ocean-to-atmosphere turbulent heat flux at high latitudes (Intergovernmental Panel on Climate Change, 1990), reduced latitudinal thermal gradient (Clark, 1990) and alteration of thermohaline circulation (Aagaard et al., 1985). The reduction in shortwave radiation transmission through sediment-laden sea ice may also significantly diminish total primary productivity underneath and within the ice cover (Horner and Schrader, 1985; Henley and Dunton, 1997).

Clay minerals typically comprise a large portion of sediments entrained in sea ice (Nürnberg et al, 1994; Naidu and Cooper, 1998; Reimnitz et al., 1998) and could affect the chemical properties of the ice cover through their adsorptive properties, primarily through reactions with contaminants and organic matter. The entrainment of such minerals into sea ice from regions of the Arctic known to be contaminated with

radioactive or other pollutants may enhance the delivery of contaminants to the central Arctic Basin and Nordic Seas (Nies et al., 1999). Entrained sediments may promote microbial activity and growth by acting as a source of macro- and micronutrients (Hedges and Keil, 1995). At the sub-centimeter scale, the spatial distribution of sediment could determine the distribution of metabolically active bacteria by localizing nutrient sources. Moreover, Measures et al. (1999) suggest that melt water from drifting sediment-laden sea ice may deliver micronutrients to large regions of the Arctic. It is likely that the adsorptive properties of sedimentary inclusions change as the sea ice cover evolves over the winter and the salinity of brine inclusions increases dramatically (Weeks and Ackley, 1986) in response to low ice-surface temperatures (as low as -35°C; Maykut, 1986).

1.7 Fate of entrained sediments

Entrained sediments may ultimately experience one of two fates: redistribution along the shelves during the following melt season, or incorporation into pack ice and transport across the Arctic Ocean by the Beaufort Gyre and Transpolar Drift (Bischof and Darby, 1997; Naidu and Cooper, 1998). Those transported into the Arctic Ocean basin may be released during summer melting, contributing to deep ocean sediments there (Clark, 1990). Given that land-derived carbon is sequestered in shelf sediments and that sea ice frequently entrains these sediments and transports them across the Arctic Ocean, it is conceivable that sea-ice rafted sediments could contribute significantly to terrigeneous carbon burial in the deep basins of the Arctic Ocean (Macdonald et al, 1998; Naidu et al., 2000).

1.8 Modeling sediment entrainment

In light of potential importance of sedimentary inclusions on the properties of the Arctic sea ice cover, it is surprising that so little research has focussed on the small-scale spatial distribution of sediments within the ice cover. Moreover, little study has related the large-scale environmental conditions that control sediment entrainment and ice growth processes to sediment concentration and the milli- to micrometer-scale distribution of entrained sediments. This study attempts to bridge the gap between large-scale environmental conditions and the small-scale distribution of sediments in sea ice.

Ideally, to link meteorological conditions to sea ice sediment concentration, one wants to determine the characteristics of bottom sediments and collect time series data on suspended sediment concentration, meteorological conditions, wave climate and ice formation. One way to accomplish this would be by deploying an instrumented tripod similar to that used by Naidu et al. (1982) to the ocean floor near a weather station that is continuously recording meteorological conditions prior to and during the freeze-up event. Sediment cores should be taken from the sea floor before freeze-up to examine the cohesiveness and grain size distribution of bottom sediments. During the freeze-up event, a time series of water samples must be collected near the tripod synchronous with the time-series wind-wave and current data. These water samples are analyzed to determine the relative concentrations of suspended material and calibrate the nephelometer, as well as to characterize the grain size distributions of the suspended material. The tripod is retrieved after the freeze-up event and the data analyzed to determine the link between meteorological conditions and sea ice sediment concentration.

However, conducting such a study is difficult due to the unpredictability of freeze-up and the potential of losing the instrument package in the harsh environment of the Arctic Ocean (Naidu et al., 1982).

An alternative approach is to use a model that has been developed to predict the resuspension of bottom sediments in shallow, coastal environments based on surface gravity wave theory and compare the model output with the sediment content of ice cores from the solidified ice cover. A semi-empirical model of wind-induced sediment resuspension has been successfully applied by Booth et al. (2000) to a microtidal, coastal environment in southern Louisiana. The model is based on equations that describe the formation and propagation of wind-induced deep-water waves. These equations have been developed by the U.S. Army Corps of Engineers, Coastal Engineering Research Center (CERC, 1984). The model predicts that bottom sediment resuspension will occur when wind-induced oscillatory wave motion reaches the floor of a water body, regardless of bottom microtopography and sediment characteristics. In order to estimate the onset of resuspension at a given point in a water body, the model compares the minimum wind velocity needed to form a wave that is capable of reaching the bottom to the actual wind velocity. Once the actual wind velocity exceeds the minimum velocity required, sediment resuspension is predicted. The model's applicability to a location is determined by qualitatively comparing the predicted resuspension potential to AVHRR-derived estimates of water turbidity.

While the resuspension model has been successfully applied to more temperate environments, a comparison is still required between the model and observational data to

determine whether the model is valid during freeze-up events (when ice crystals are present in the water and AVHRR data are unreliable) or not. The unpredictability and potentially dangerous conditions of freeze-up events make direct observation difficult. On the other hand, indirect evidence of conditions during freeze-up events (e.g., seawater sediment concentrations, presence or absence of a turbulent water column) can be obtained through the analysis of ice cores extracted from the solidified ice cover. Ice coring offers fewer time constraints and is much less hazardous. Although other processes may affect the sediment content of the ice cover after freeze-up events, observational data from ice cores should still indicate the relative importance of sediment resuspension in sediment entrainment. Due to the difficulties involved in obtaining time series data of wave climate and water samples during freeze-up, the study presented here used the modeling and ice coring approach to obtain estimates of the onset of sediment resuspension.

In this study, the relationship between environmental conditions and the sub-centimeter-scale spatial distribution of sedimentary inclusions was determined through a three-part process. First, the sediment resuspension model discussed above was employed to examine the relationship between meteorological conditions present during freeze-up and the large-scale spatial and temporal variability of sedimentary inclusions resulting from sediment entrainment. Second, the small-scale spatial distribution of sedimentary inclusions were linked to sea ice type and large-scale distribution of sediment content through the examination of samples of the seasonal sea ice cover near Barrow, Arctic Alaska, USA, formed during the fall 1998, 1999 and 2000 freeze-ups.

While the sediment content was measured using the conventional melt/filter method, the spatial distribution of sediments in the ice cover was determined by a new non-destructive, optically-based method. Finally, a link was proposed between the environmental conditions prevailing during fall freeze-up and the resulting small-scale spatial distribution of sediments within the sea-ice cover. Figure 3 illustrates the position of the current study and its components with respect to various processes.

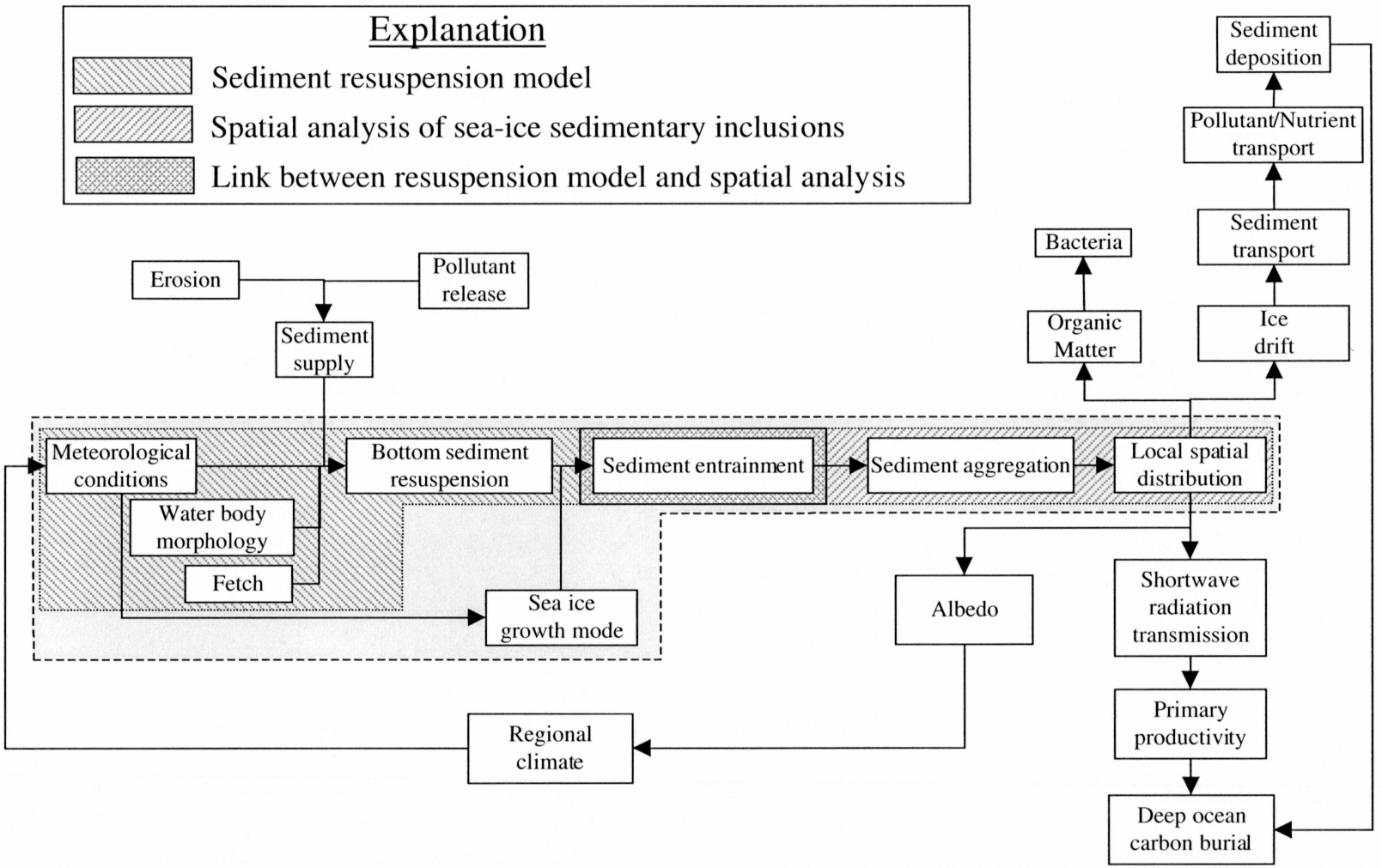

Figure 3. Relationship of sediment entrainment processes to other processes. The gray box represents those parameters and processes examined in this study.

Chapter 2

Study Area, Materials and Methods

2.1 Study area

The study area was far western Elson Lagoon, located 13 km northeast of Barrow, Alaska, USA (Figure 4). The lagoon is bounded on the northwest and northeast by barrier islands that extend two- to three-meters above sea level, while the coastal plain of the North Slope of Alaska forms the southwest and southeast coastlines. The lagoon averages 7 km wide and 56 km long and is less than 4 m deep. The lagoon floor is composed primarily of unconsolidated muddy sediments, but exposed cobbles have been observed near Eluitkak Pass (E. Reimnitz, pers. comm.). The tidal range is less than 16 cm.

2.2 Modeling sediment resuspension

Previous studies of sediment inclusions in Arctic sea ice suggest that spatial variability in sediment load exists (e.g., Osterkamp and Gosink, 1984; Reimnitz et al., 1993; Nürnberg et al., 1994). In attempting to explain such variability as the result of local environmental conditions governing resuspension and hence entrainment of particles, this study employed the resuspension model developed by Booth et al. (2000). Similarities between Elson Lagoon and the environment for which the resuspension model was developed (a shallow, microtidal, coastal environment with unconsolidated, fine-grained bottom sediments) justify the use of this model. The resuspension model was applied to the study area for days during the onset of fall freeze-up.

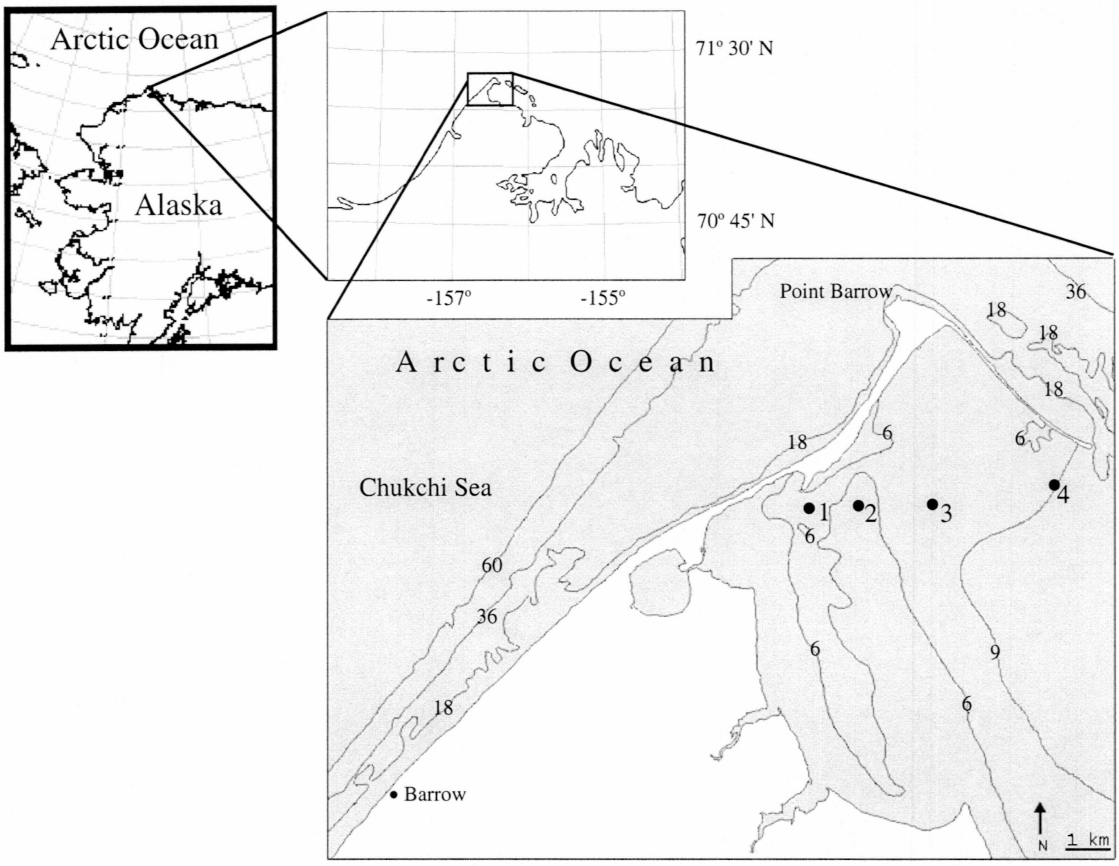

Figure 4. Sea ice coring locations in Elson Lagoon near Barrow, AK. Samples were taken from site 1 in 1999 and 2001, while samples were taken from sites 1 - 4 in 2000. Table 1 lists the corresponding site designations referred to in the text. Bathymetry is in feet.

Site	Year	Location	Length (cm)
9903-10	1999	1	113
0005-1	2000	1	32
0005-2	2000	2	39
0005-3	2000	3	86
0005-4	2000	4	49
0104-1	2001	1	10

Table 1. Site designation, year of extraction, location (Figure 4) and core length.

As previously indicated, the resuspension model predicts that sediment resuspension occurs when wind-induced oscillatory wave motion reaches the floor of a water body. For resuspension to occur, a critical wavelength (L) of 2d (where d is water depth) must be generated (Pond and Pickard, 1983). The critical wavelength is related to wave period (T) by (CERC, 1984)

$$L = gT^2 / 2\pi,$$

where g is the acceleration due to gravity (9.8 m/s^2). Assuming a wind duration of 24 hours, wave period is related to wind velocity (U) and fetch (F) by (CERC, 1984)

$$gT / U_A = 0.2857(gF / U_A^2)^{1/3},$$

where the wind stress factor, U_A, is related to wind velocity by

$$U_A = 0.71(UR_T)^{1.23}.$$

R_T is a boundary layer stability correction factor and is often taken to equal 1.1 (CERC, 1984). From these equations, a critical wind velocity necessary to suspend bottom sediments is determined. The resuspension potential at a given location is the difference between the actual wind velocity and the critical wind velocity.

The model requires only a few input parameters, including 24-hour resultant wind velocity, bathymetry and fetch. July, August and October meteorological data for Barrow (National Climatic Data Center, http://www.ncdc.noaa.gov) were used in the model, as this was the closest National Weather Service station (13 km from the study site). The shoreline and bathymetry of Elson Lagoon were digitized from 1:63,360 topographic maps (United States Geological Survey, 1955). The fetch was calculated for eight dominant wind directions at all locations in the study area and subsampled to a grid

with a point spacing of 165 m for use in the ArcInfo (ESRI, Redlands, CA) software package. Values of resuspension potential were then calculated for dates during the initiation of freeze-up from the meteorological, bathymetric and fetch data for each grid point, by running the resuspension model's equations through ArcInfo.

To assess the applicability of the resuspension model to Elson Lagoon, model runs during the ice-free season were qualitatively compared to satellite-derived relative estimates of turbidity as outlined by Booth et al. (2000). The following modifications were made to account for the potential of a sea-ice cover and the use of the TerraScan (SeaSpace Corp., Poway, CA) and ArcInfo software packages in place of the ENVI (Research Systems Inc., Boulder, CO) software package. Advanced Very High Resolution Radiometer (AVHRR) level 1b High Resolution Picture Transmission (HRPT) imagery was collected from the National Oceanic and Atmospheric Administration's Satellite Active Archive (http://sit.saa.noaa.gov/) for those ice-free days when little or no cloud cover was present over the study area (July and August). The images were georeferenced and converted to percent reflectance by applying the auxiliary parameters outlined in Di and Rundquist (1994) using the TerraScan software package. The images were not ground-truthed. ArcInfo was then used to compare the percent reflectance of each pixel along a transect across each image to the resuspension potential value of a point corresponding to the center of the pixel.

2.3 Spatial analysis of sea ice sediment inclusions

Up to this point, studies have focused primarily on the variability of total sediment load and few have considered sedimentary inclusions at scales in the micro- to millimeter

range. Here, we examine sub-centimeter-scale parameters that are relevant in the context of the effect of particulates on optical properties and microbial life in sea ice. We determine the spatial and temporal distribution of sedimentary inclusions by examining sea-ice samples at two different scales.

Sea ice cores were extracted from western Elson Lagoon on March 14, 1999, May 9, 2000, and April 3, 2001 at the locations shown in Figure 4. During the 1999 sampling period air temperatures remained near -30°C or -40°C, with the ice surface at temperatures between -15°C and -20°C (Eicken et al., 2000b). During the 2000 sampling period both air and ice surface temperatures were approximately -5°C. During the 2001 sampling period air temperatures ranged from -15°C to -25°C and the ice surface temperature was -15°C.

A total of 11 cores were collected for the purpose of this study, two at Station 1 in 1999, two each from Stations 1 through 4 in 2000 and one from Station 1 in 2001. Five additional cores were extracted from the ice cover at various locations in 2001, but these cores contained too little frazil ice to include them in the analysis. The cores were extracted from the sea ice cover using a 10 cm-diameter CRREL-type fiberglass-barrel auger. Only the frazil ice layer of each core was analyzed in this study. Table 1 lists the core locations and the length of the frazil ice segments. After extraction, one core from each site (except for the core from 2001) was maintained at close to in-situ temperature during storage and transport to Fairbanks, AK. There, they were stored at -15°C prior to analysis. The remaining cores (including the core from 2001) were cut into 5 to 10 cm segments lengthwise on site and later melted. The melt water from each segment was

then filtered through a 1.0-μm A/E glass fiber filter (Gelman Sciences) to collect the entrained sediment and the filters stored at -15°C prior to analysis. The filtered samples were weighed after they were dried overnight at 50°C.

Two different types of sea-ice samples were prepared from the intact cores, one for microscopic and the other for macroscopic examination. Ice sections (2 cm x 2 cm x 5-6 mm thick) for microscopic examination were prepared as outlined in Junge et al. (2001). These sections were examined under both transmitted and cross-polarized light using a cold-adapted Zeiss Axioskop 2 microscope with a 20x objective connected to the digital camera setup described below. On-screen magnification was 1025x. Each microscopic field of view covered an area of 0.041 mm^2 and had a focal depth of 0.02 mm. Two to four transects, typically 80 microscopic fields long, were conducted across each sample and all fields containing sedimentary inclusions were captured and analyzed. The total number of fields scanned in each transect was noted. Image analysis consisted of outlining each sedimentary inclusion and determining the length of the minor axis of an inscribed ellipse.

All images were acquired using a MTI DC330E 3CCD color camera in conjunction with a Scion CG-7 RGB Color PCI frame grabber. This combination produced a total image size of 768 by 576 pixels. A variant of NIH Image v. 1.62c (Rasband and Bright, 1995), running on a G3 Macintosh with 128MB RAM, was employed in the image acquisition, calibration, analysis and display steps.

Vertical thin sections (5 cm x 5 cm x ~0.5 mm thick) for macroscopic examination were processed as described by Eicken and Lange (1991), with the exception of cores

9903-10 and 0005-1. Due to mechanical difficulties, thin sections from these two cores were microtomed to an approximate final thickness of 1.5 mm rather than 0.5 mm. For sedimentary particle analysis, images of the thin sections were acquired using a Canon 28mm-80mm macro-lens connected to the digital camera setup described above. Illumination was provided by a fluorescent light table. On-screen magnification was 12.3x and each pixel represented a linear dimension of 0.026 mm. Each thin section was imaged in a mosaic format with no overlap between adjacent images, producing nine images per sample on average. The resulting three-channel images were then contrast-enhanced. Image segmentation was achieved using the unsupervised, maximum-likelihood, multi-spectral classification scheme in MultiSpec v. 4.2.00 (http://dynamo.ecn.purdue.edu/~biehl/MultiSpec/; running on the Macintosh G3 described above) with the number of classes preset to 15. Presetting the number of classes to 15 resulted in one class that consistently corresponded to sedimentary inclusions. Visual verification of the classification results indicated that this method was sensitive to the presence of relatively large air pockets and brine pockets that were intercepted and filled with ice shavings during microtoming. These shaving-filled pockets were often misclassified as sedimentary inclusions by the classification scheme. However, such pockets were easily identified by visual inspection of the thin sections and were removed from the classification output of samples from sites 0005-1 and 0005-2. Compressed air was used to remove the shavings from all other samples before imaging. The number density and cross-sectional areas of sedimentary inclusions (aggregates) were determined from the classification output. Nearest neighbor distances between

aggregates were measured by performing successive non-linear or morphological filters ("dilations"; neighborhood pixel count = 1, iterations = 1) and counting the number of remaining "aggregates" after each dilation. Finally, the 'nearest-neighbor test for clustering and regularity' was performed using the measured nearest neighbor distances (Swan and Sandilands, 1995). The results of this vertical thin section analysis were grouped for each 10 cm length of core (i.e., 0-10 cm, 10-20 cm, etc.) to facilitate comparison to the gravimetric results derived from 10 cm core segments.

A qualitative assessment of ice stratigraphy was made from images of the thin sections between crossed polarizers acquired with an Olympus D-500L digital camera. Illumination was provided by a fluorescent light table. Onscreen magnification was 2.9x.

A simple geometric model was used to explore the relationship between the spatial distribution and concentration of sediments in the ice cores. Given the following assumptions:

(1) mass density of entrained lithologic particles is uniform

(2) aggregates of the particles exhibit a constant porosity

(3) aggregates are spherical

(4) there is a random spatial distribution of aggregates within the ice

it should be possible to estimate sediment concentration based on measured mean aggregate cross-sectional area and aggregate number density. The proposed model has the form:

$$S = A\left[\frac{4\pi}{3}\left(\frac{x}{\pi}\right)^{1.5}\right]y + C$$

where:

S = sediment concentration (mg/l)

A = volume-to-concentration conversion coefficient (mg/l)

x = mean aggregate cross-sectional area (mm^2)

y = mean aggregate number density (mm^{-3})

C = constant (mg/l)

The constant "C" represents an estimate of the sediment concentration not accounted for due to the lower limit of resolution of the imaging system.

Chapter 3

Results

3.1 Modeling sediment resuspension

The results from the assessment of the resuspension model's applicability to Elson Lagoon are shown in Figure 5. According to Booth et al (2000), resuspension potentials of zero or less represent areas where no bottom-sediment resuspension is predicted to occur, while positive resuspension potentials suggest that resuspension of bottom sediments is taking place. In Figure 5, relatively low percent reflectance values (<5.8%) correspond to resuspension potentials of zero or less. Higher percent reflectance values (>5.8%) coincide with resuspension potentials greater than 5. However, the lack of a definite trend between -2 and +5 makes it difficult to detect the precise resuspension potential at which resuspension commences. Nevertheless, good agreement between the resuspension potential and the AVHRR-derived relative turbidity outside of this interval suggests that the resuspension model is appropriate for Elson Lagoon.

Predicted bottom-sediment resuspension potentials for the fall freeze-up periods corresponding to the spring 1999, 2000 and 2001 sampling seasons are shown in Figure 6. Resuspension potential values and corresponding average sediment loads for specific sampling sites are listed in Table 2. The fall 1998 and 2000 freeze-up periods (corresponding to 1999 and 2001 samples, respectively) were characterized by relatively light winds and low resuspension potentials (less than +8) over much of the study area. On the other hand, during the fall 1999 freeze-up (corresponding to 2000 samples), relatively high wind stress and a long fetch resulted in resuspension potentials in excess

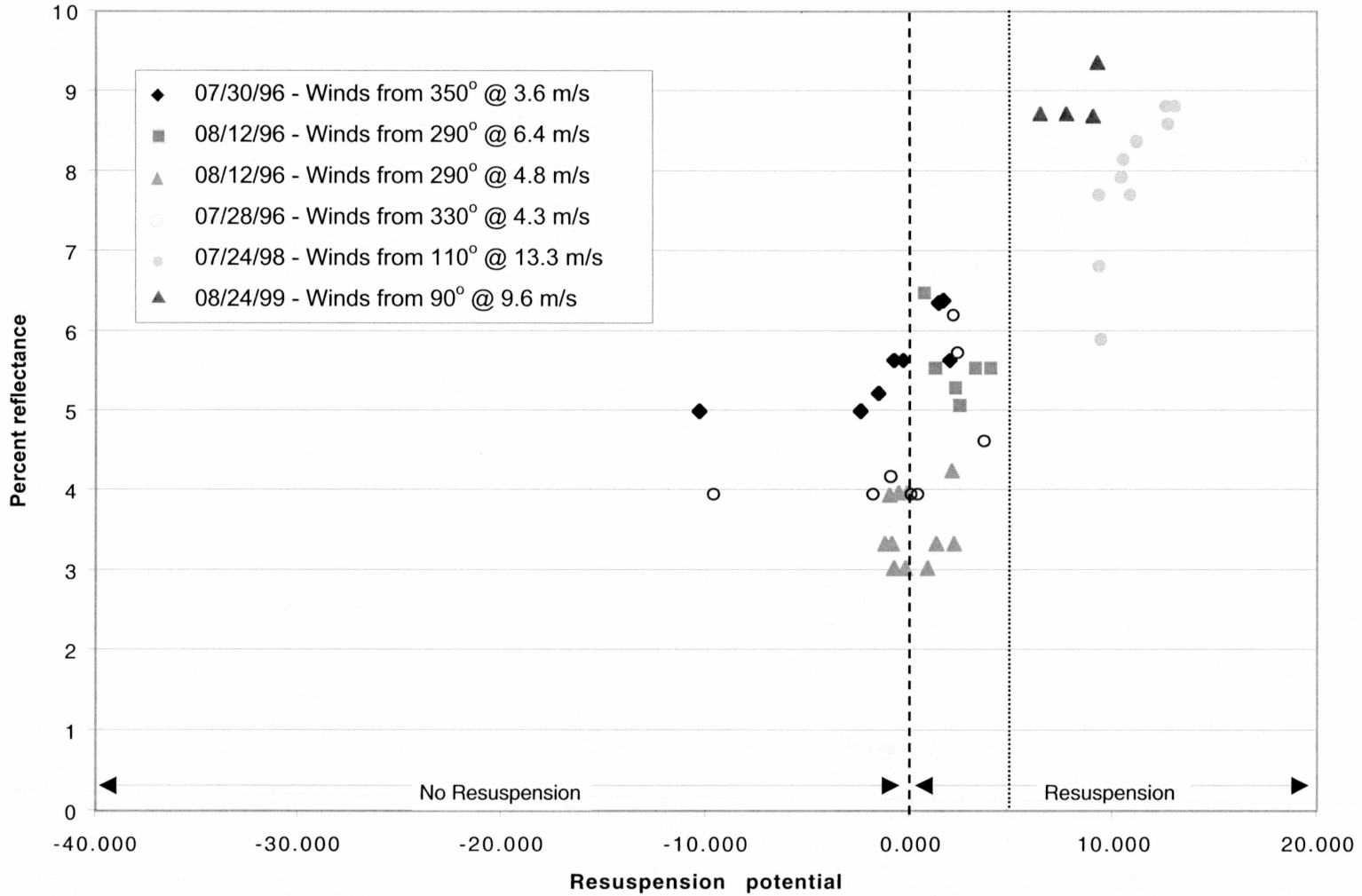

Figure 5. Assessment of the resuspension model's applicability to Elson Lagoon. This chart shows the relationship between the AVHRR modified channel 1 percent reflectance and the modeled resuspension potential. Note the increase in percent reflectance values at resuspension potentials greater than ~+5 (dotted line).

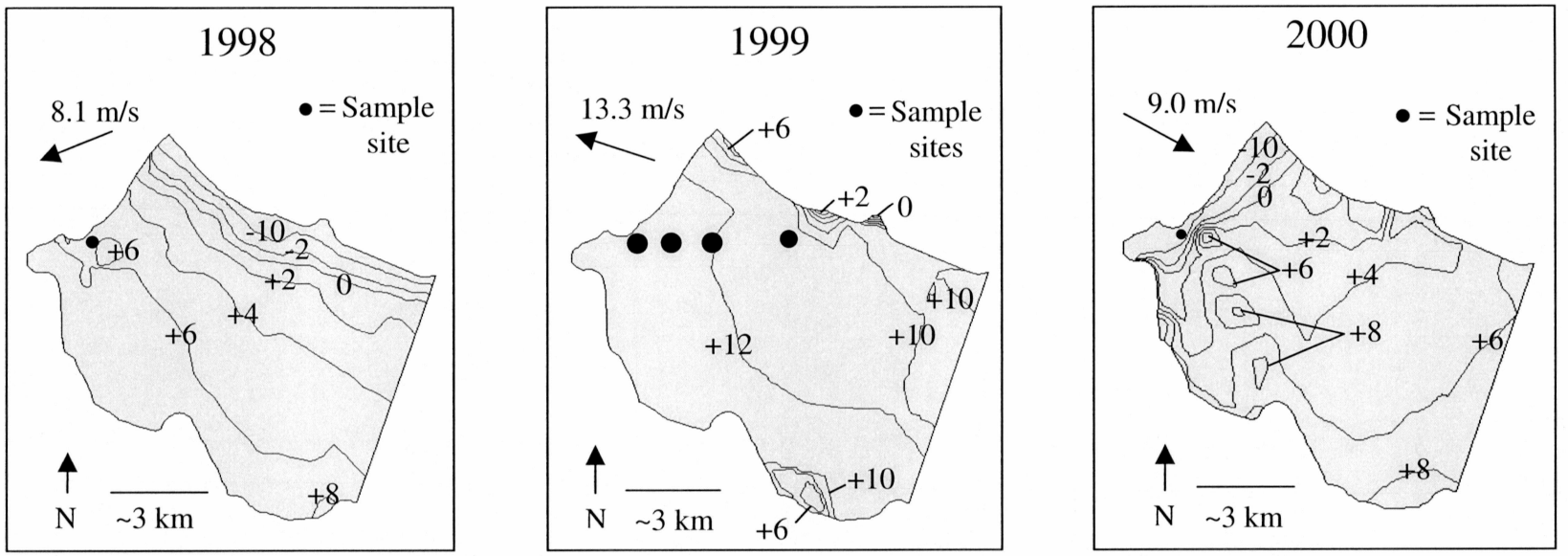

Figure 6. Maps of sediment resuspension potential for the 1998, 1999 and 2000 fall freeze-up events. These freeze-up events correspond to the spring 1999, 2000 and 2001 sampling seasons referred to in the text, respectively. Sample sites are the locations indicated on Figure 2 for each of the three sampling seasons. Relative sediment load at each site is indicated by dot size. Wind speed and direction are indicated in the upper left corner of each figure. The contour interval is 2 down to -2. To enhance readability, below -2 only the -10 contour is marked.

Site	Sediment load of frazil ice layer (g/m^2)	Resuspension potential
9903-10	59	5.5
0005-1	348	12.6
0005-2	338	12.5
0005-3	384	12.2
0005-4	262	10.2
0104-1	2	-74.7

Table 2. Sediment load and resuspension potential for each sampling site.

of +10 over most of the study area. The predicted resuspension potential corresponding to site one was 2.3 times greater in 1999 (core 0005-1) than in 1998 (core 9903-10). The model predicted no resuspension at site one in 2000 (core 0104-1). The trend in average sea ice sediment load among the three years is similar to that of resuspension potential, with core 0005-1 having an average sediment load six times greater than core 9903-10 and 174 times greater than core 0104-1. Thus, there is qualitative agreement between the resuspension model and the sea ice sediment load.

3.2 Analysis of sea ice

Sub-meter-scale observations of sea ice samples from the study area reveal a patchy distribution of sediments (Figure 7). Regions of high sediment concentrations are frequently interspersed amongst regions of low sediment concentrations at larger scales. At microscopic scales, sediment appears to be concentrated in brine inclusions rather than in the ice matrix.

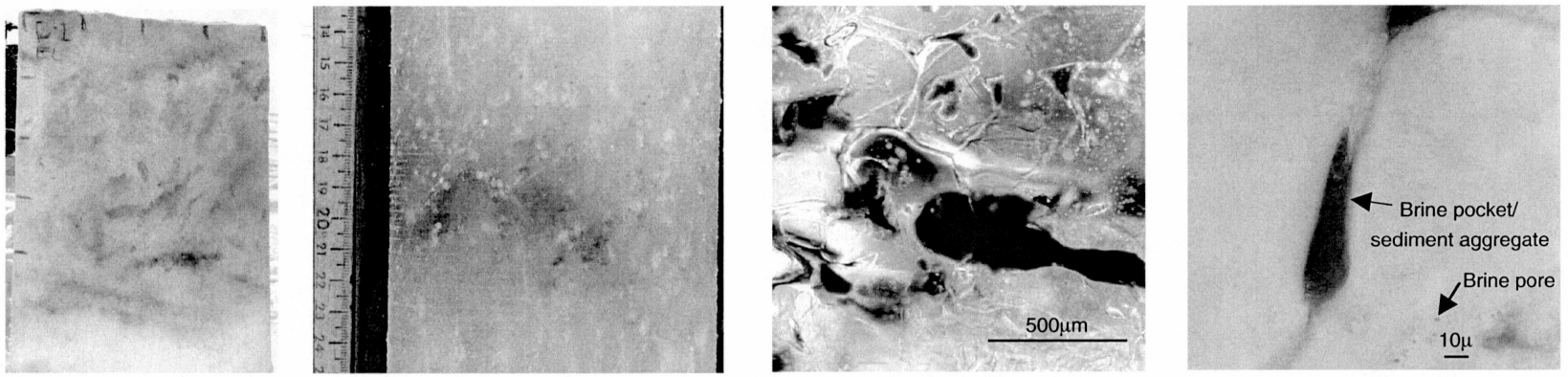

(a) (b) (c) (d)

Figure 7. Distribution of sediment inclusions over a range of scales. A sequence of images showing the spatial distribution of sediment and structural features over a range of scales in sea ice samples acquired in March 1999. The black marks along the top and left edges of (a) are spaced approximately 10 cm apart. Note meter stick in (b) for scale.

Figure 8 shows two images of ice crystals that are representative of all core segments analyzed. These crystals are predominantly small (< 10 mm diameter), equant to prismatic in shape and have irregular outlines, typical of frazil ice. Moreover, while vertically oriented grain-boundaries are frequently observed in the upper 10-20 cm of each core (Figure 8a), there is no evidence of the large, columnar crystals representative of congelation ice growth (Weeks and Ackley, 1986) in the uppermost, sediment-laden layers. Below, however, crystals are almost exclusively of the typical vertically elongated (up to >10 cm long) columnar shape with numerous intra- rather than intercrystalline brine inclusions. This observation was confirmed by detailed microstructural and stratigraphic analyses as part of another study at the same site (D. Cole, pers. comm.).

3.3 Spatial characteristics of sediment inclusions

Table 3 lists the results of the gravimetric, macroscopic and microscopic analyses. Gravimetric sediment concentrations range from 23.9 mg/l to 1474.3 mg/l. The lowest concentrations occur in core 9903-10, while the highest concentrations are found in cores 0005-1 and 0005-2. The average sediment concentration of core 0005-1 is eight times larger than that of core 9903-10.

Descriptors of the small-scale spatial distribution of sedimentary aggregates in the sea ice samples show a high degree of variability. Aggregate number densities span two orders of magnitude, from 0.01 to 3.55 mm^{-3} (mean = 0.83 $mm^{-3} \pm 0.74$ mm^{-3} (1σ)), with

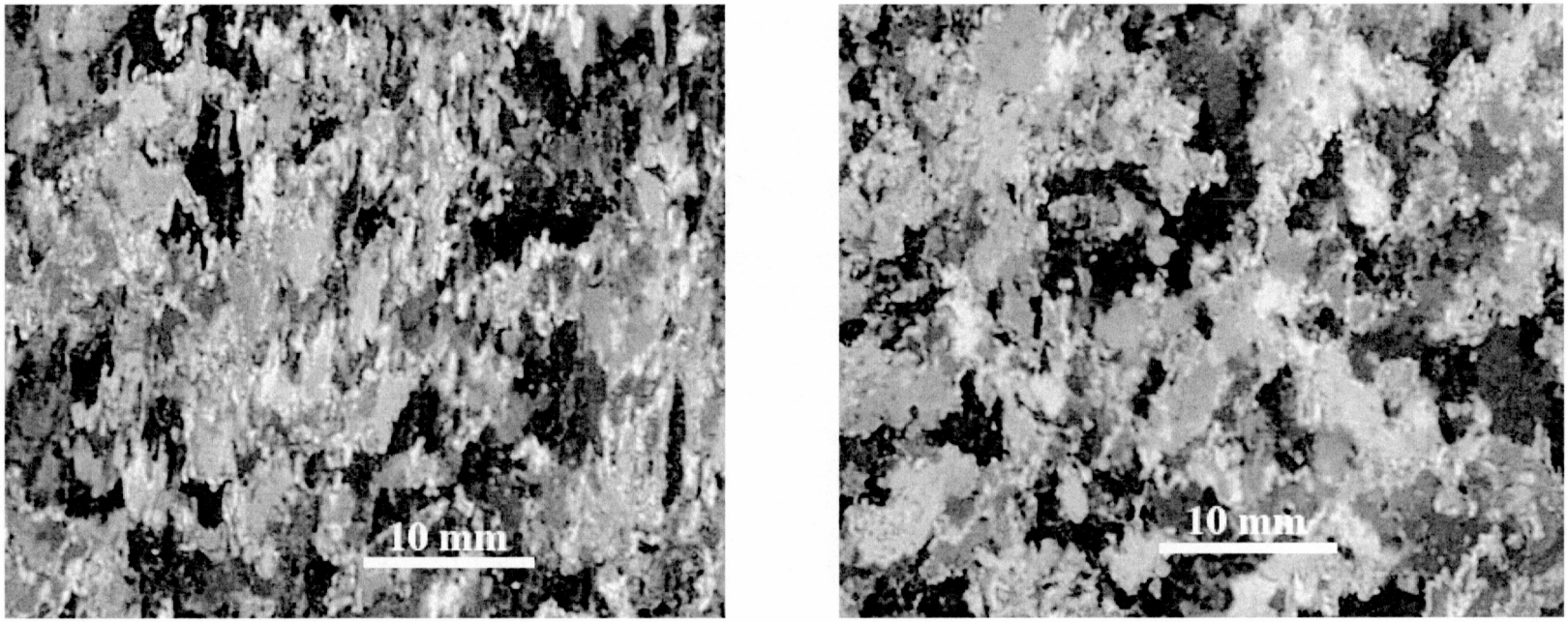

(a) (b)

Figure 8. Images of the vertical sea ice structure. These images show the morphology of ice crystals near the top and bottom of core 0005-2 (a = segment 0-5 cm, b = segment 30-35 cm). The thin section images were taken between crossed polarizers. Note the predominance of small, subequant ice crystals in both images and their irregular outlines.

			Macroscopic image analysis				Microscopic image analysis	
Site	Depth interval (cm)	Gravimetric sediment load (mg/l)	Aggregate number density (mm^{-3})	Mean aggregate cross-sectional area (mm^2)	Mean nearest-neighbor distance (mm)	Nearest-neighbor statistic	Aggregate number density (mm^{-3})	Mean aggregate width (mm)
9903-10	0-10	23.9	0.01	0.0013	2.33	0.617		
	10-20	76.0	0.04	0.0029	1.41	0.759		
	20-30	199.0	0.02	0.0025	1.65	0.535		
	30-40[1]	275.1	0.16	0.0084	0.60	0.622	112	0.0271
0005-1	0-10	604.6	0.38	0.0028	0.48	0.682	381	0.0087
	10-20	1474.3	0.66	0.0062	0.34	0.734		
	20-30	1416.6	0.38	0.0082	0.42	0.775		
0005-2	0-10	276.4	1.07	0.0034	0.43	0.814		
	10-20	1457.1	1.35	0.0063	0.43	0.775		
	20-30[2]	1119.4	3.55	0.0053	0.33	0.713		
	30-40	477.8	0.85	0.0018	0.53	0.815		
0005-3	0-10	434.2	0.42	0.0018	1.05	0.888		
	10-20	421.7	0.75	0.0022	0.90	0.899		
	20-30	420.7	1.02	0.0019	0.88	0.916		
	30-40	489.2	0.54	0.0028	0.85	0.886		
	40-50	386.7	0.99	0.0025	0.73	0.894		
	50-60	434.6	1.05	0.0034	0.71	0.866		
	60-70	752.4	0.65	0.0039	0.71	0.866		
0005-4	0-10	405.4	0.73	0.0016	0.69	0.838		
	10-20	637.4	1.04	0.0026	0.70	0.910		
	20-30	320.4	1.24	0.0033	0.51	0.823		
	30-40	843.1	1.28	0.0034	0.44	0.818		
0104-1	0-10	26.2						

Table 3. Results of the gravimetric, macroscopic- and microscopic-image analyses. The site designations correspond to the locations indicated in Figure 4. 1 = core segment excluded from further analysis due to an unusually large mean aggregate cross-sectional area. 2 = core segment excluded from further analysis due to an unusually large aggregate number density.

the core from 1999 (9903-10) having number densities approximately one order of magnitude lower than cores from 2000. Results of a two-sample t-test indicate that the aggregate number density is significantly lower ($P<0.05$) in 1999 core samples (mean = 0.05 $mm^{-3} \pm 0.07$ mm^{-3}) than in 2000 core samples (mean = 0.99 $mm^{-3} \pm 0.71$ mm^{-3}). Significant variability in aggregate number densities also exists within each core as demonstrated by a two- to 16-fold difference between the smallest and largest number densities in each core.

Mean aggregate cross-sectional areas and nearest-neighbor distances show a high degree of variability, as well. Mean aggregate cross-sectional areas vary by a factor of six, from 0.0013 to 0.0084 mm^2. Samples from 1999 tend to occupy the lower part of this range, while samples from 2000 cover almost the entire range of values. Individual cores exhibit two- to six-fold differences between minimum and maximum cross-sectional areas. Mean nearest-neighbor distances also span a six-fold range of values from 0.33 to 2.33 mm, with much of this variability coming from the 1999 core. Three of the segments from core 9903-10 exhibit distances between 1.5 and 7 times those found in samples from 2000.

The nearest-neighbor statistic is much less variable, with values falling between 0.54 and 0.92. Results of a two-sample t-test indicate that the nearest-neighbor statistic is significantly lower ($P<0.05$) in samples from 1999 (mean = 0.63 ± 0.09) than in samples from 2000 (mean = 0.83 ± 0.07). Swan and Sandilands (1995) state that the nearest-neighbor statistic can vary from 0 (all points coincident) to 2.15 (equally spaced points). Clustered distributions are represented by low values, random distributions by

intermediate values and equally spaced distributions by high values (Figure 9). Thus, collectively, all samples appear to exhibit a random spatial distribution of particles, but with some tendency toward clustering. More specifically, samples from 1999 exhibit a more clustered spatial distribution than samples from 2000.

In all further analyses of the macroscopic data, the 30-40 cm segment of core 9903-10 and the 20-30 cm segment of core 0005-2 have been excluded. The first segment has been excluded because the mean aggregate cross-sectional area is three times greater than that of other segments with similar sediment concentrations. Visual inspection of this segment revealed atypically large and elongated sediment inclusions in comparison to other ice segments. The mechanism responsible for including such unusual aggregates into the frazil ice layer is unknown, but the incorporation of anchor ice is a possibility. The second segment has been excluded, because the mean aggregate number density for this segment appears to be an outlier (3.7 standard deviations away from the mean). It is unclear why the aggregate number density of this segment is so much higher than that of other segments with similar sediment concentrations (Table 3 and Figure 10).

Some macroscopic, optically-derived parameters exhibit positive correlations with sediment concentration, while others do not. Regressions of mean nearest-neighbor distance and mean aggregate cross-sectional area against sediment concentration yield R^2 values of 0.78 and 0.82, respectively ($P<0.01$, Figure 11). However, aggregate number density does not exhibit a significant correlation with sediment concentration ($R^2 = 0.09$, $P>0.05$, Figure 10).

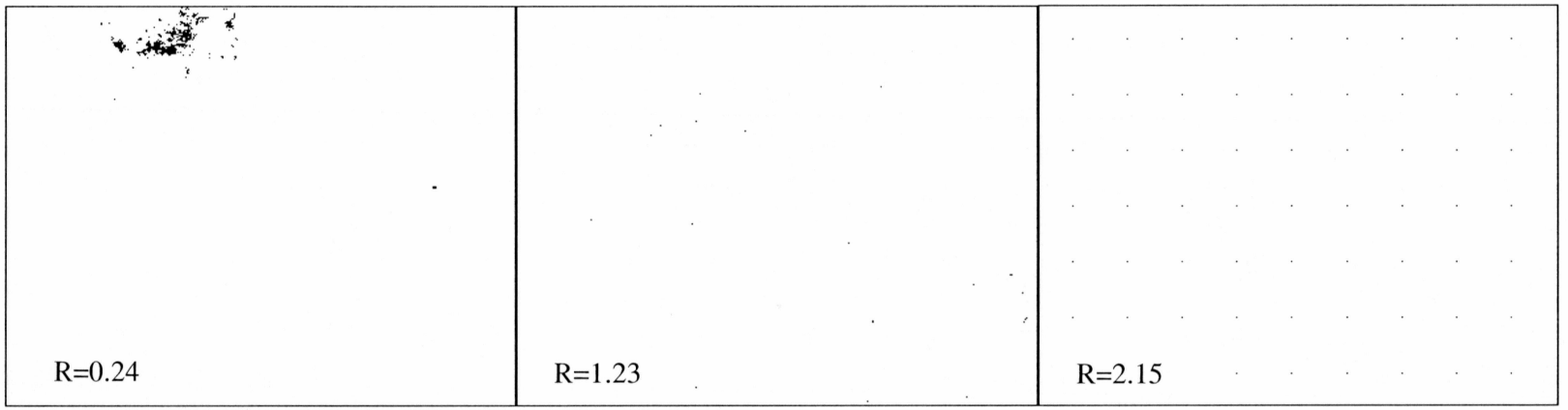

Figure 9. Spatial distributions exemplified by the nearest-neighbor statistic, R. Highly clustered distributions are indicated by low R values (left image), random distributions correspond to intermediate R values (center image), and uniform distributions are represented by high R values (right image).

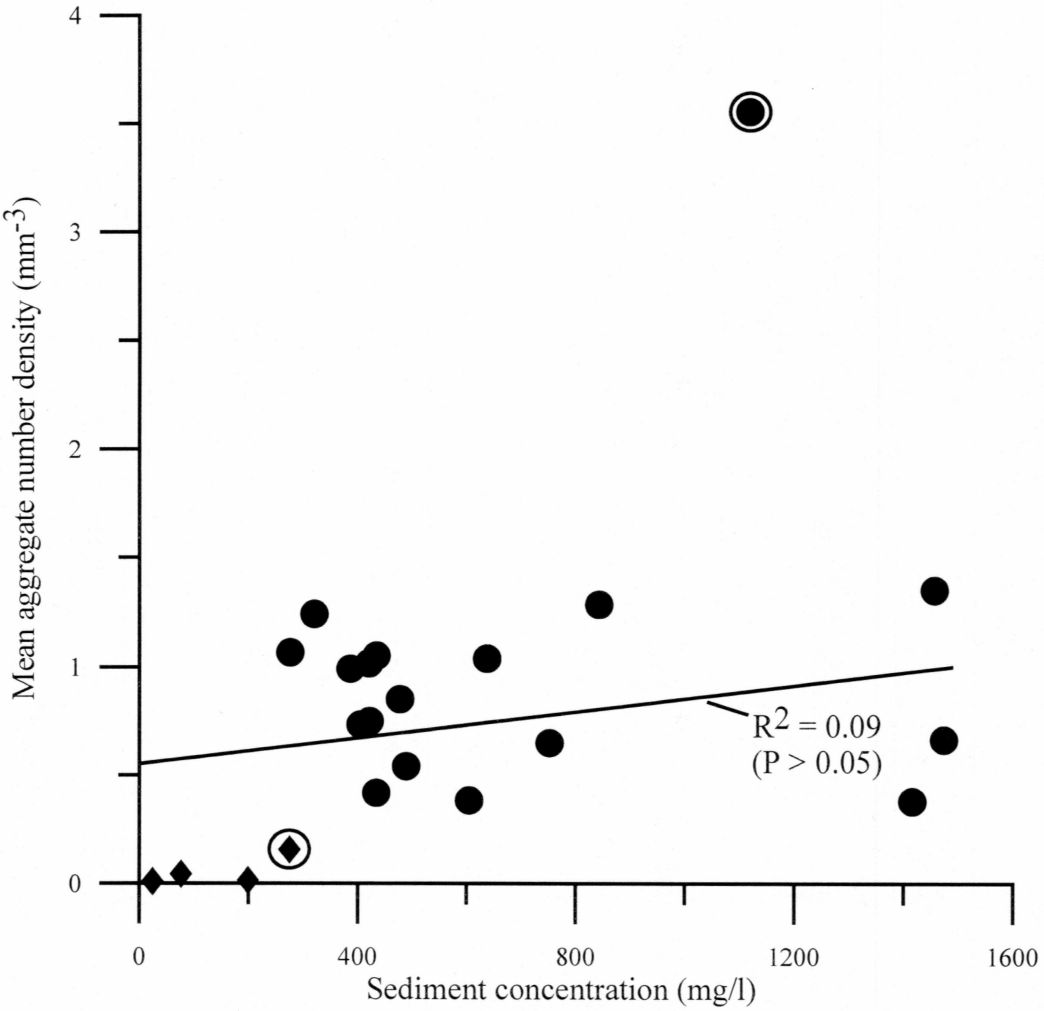

Figure 10. Relationship between sediment concentration and mean aggregate number density. Diamonds represent samples acquired in 1999 and filled circles represent samples acquired in 2000. Circled values correspond to the 9903-10 (30-40 cm) and 0005-2 (20-30 cm) core segments, which were excluded from the regression analysis. Note that the regression line is not significant at the 95% confidence level.

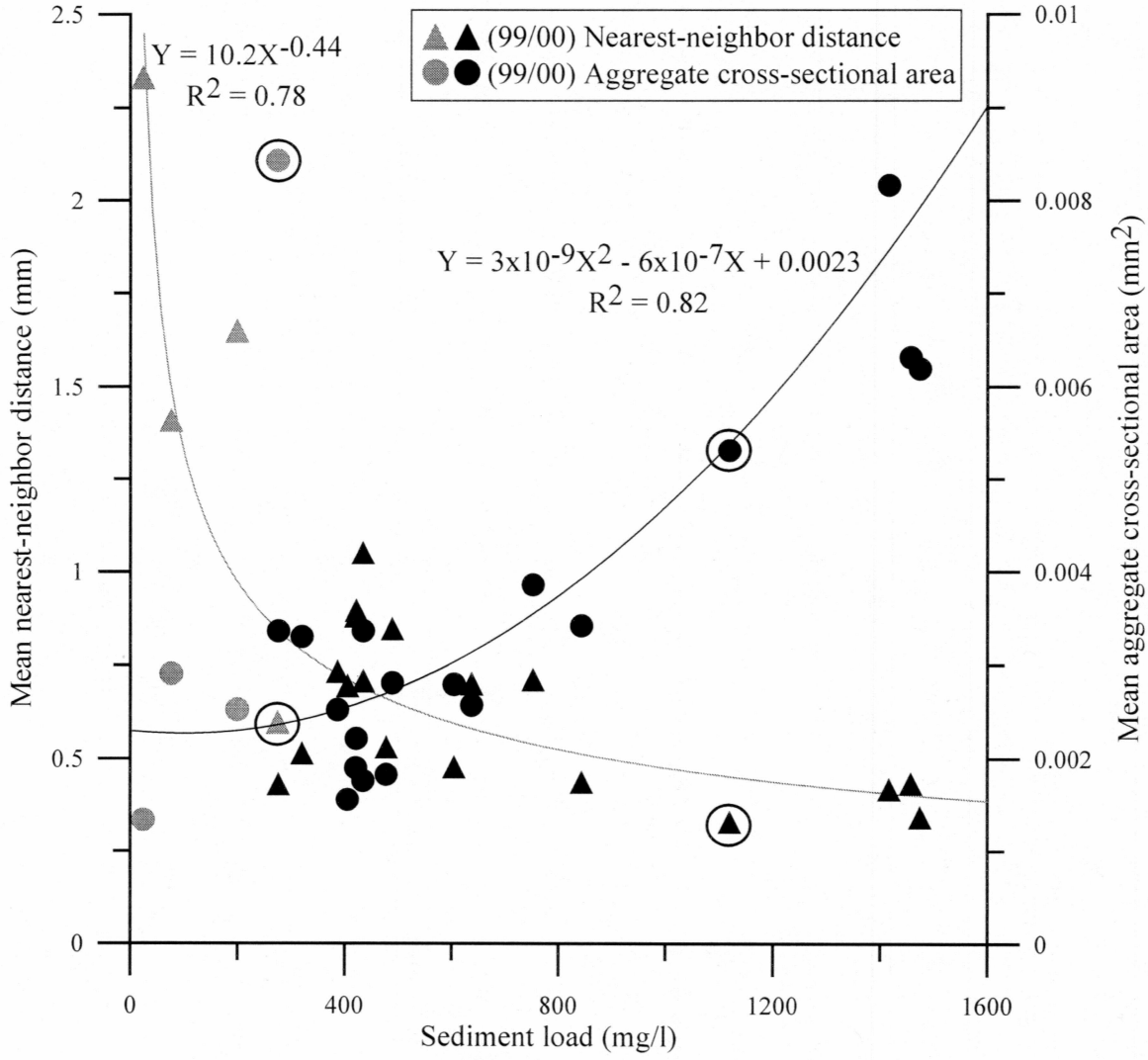

Figure 11. Relationships between sediment concentration and mean nearest-neighbor distance and mean aggregate cross-sectional area. The circled data points represent samples 9903-10 (30-40 cm) and 0005-2 (20-30 cm) and were excluded from the regression analyses.

Figure 12 illustrates the relationship between the mean aggregate cross-sectional area and mean aggregate number density and sediment concentration. The best-fit geometric model ($R^2 = 0.61$, $P<0.01$) is:

Sediment concentration (mg/l) = $2.8x10^6$ mg/l * [4/3 * π * (mean aggregate cross-sectional area/π)$^{1.5}$] * (mean aggregate number density) + 260 mg/l.

Table 3 shows the results of the microscopic image analysis. A total of 17 transects were examined from Elson Lagoon ice samples. The length of time required to prepare samples and collect enough data for statistically significant results precluded analyzing more depth intervals. The transects yielded 103 sedimentary aggregates in 1999 and 90 in 2000. The aggregate number density in the 2000 sample is 3.4 times greater than in the 1999 sample, a trend similar to that observed in the macroscopic analysis. Microscopic aggregate number densities are approximately three orders of magnitude larger than those determined using the macroscopic imaging technique. This is to be expected, since the magnification used in the microscopic analysis was almost two orders of magnitude greater than that used in the macroscopic analysis. Average aggregate width is 3.1 times greater in the 1999 sample than in the 2000 sample. Again, the relationship between the years is similar to that observed in the macroscopic analysis of mean cross-sectional area. Although the two dimensions are not directly comparable, they are nevertheless related if one assumes approximately spherical aggregates. All sedimentary aggregates identified in the microscopic image analysis occupied brine inclusions, usually in brine pockets and triple junctions.

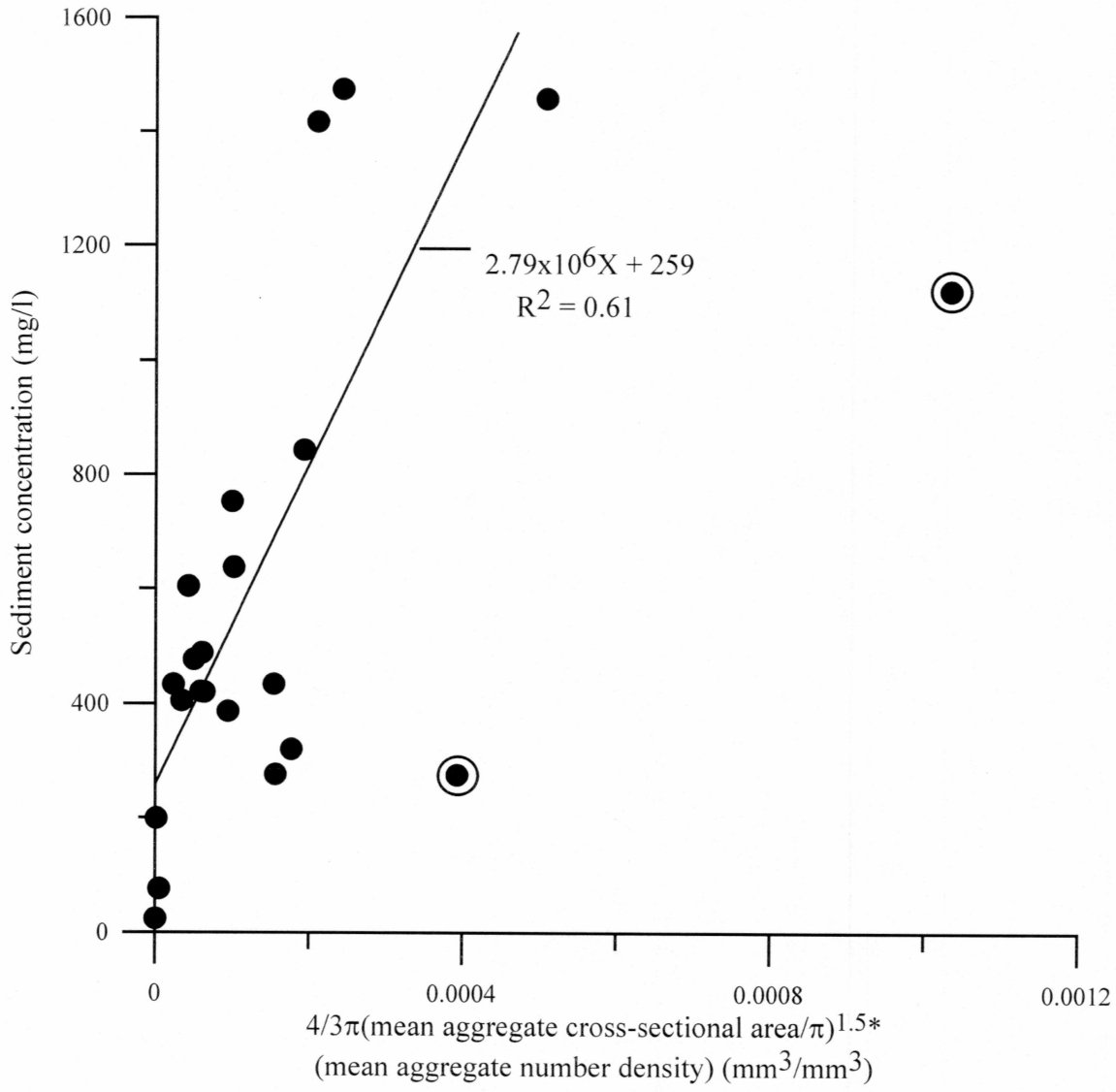

Figure 12. Best-fit geometric model relating mean aggregate number density and mean aggregate cross-sectional area to sediment concentration. The circled data points represent samples 9903-10 (30-40 cm) and 0005-2 (20-30 cm) and were excluded from the regression analysis.

Chapter 4

Discussion

The multi-scale approach employed in this study yielded a number of significant results. Meteorological conditions at the time of freeze-up are important factors determining bulk sediment content and the spatial distribution of sediments within the sea ice cover. Processes responsible for sediment entrainment and sea ice formation in Elson Lagoon are similar and depend on only a few environmental parameters, namely water depth, fetch and wind velocity (assuming a wind duration of 24 hours). Significant natural variability exists both spatially and temporally within the sea ice cover.

4.1 Modeling sediment resuspension

Sediment resuspension in shallow marine environments occurs when sufficient tangential stress is applied to the sediment-water interface to dislodge and entrain sediment into the water column (Komar and Miller, 1973). The amount of tangential stress required to dislodge sediment is a function of the size and density of grains, cohesive forces acting between sedimentary particles and the drag coefficient of the bottom. The total stress available for a unidirectional flow is a function of fluid viscosity, water parcel velocity and acceleration and hydrodynamic roughness of the sediment-water boundary. If one assumes that sediments in Elson Lagoon are predominantly fine-grained (mostly silt and clay), of similar density and cohesiveness, and suspended in seawater of constant density, then the potential for sediment resuspension is dependent on water parcel velocity and acceleration. The velocity and acceleration of water parcels are determined by ocean currents generated by tides, thermohaline circulation and surface

winds, among other factors. Studies in shallow Arctic regions show that increases in water-column sediment concentration frequently coincide with the occurrence of strong surface winds, suggesting that wave-induced oscillatory currents are important in resuspending bottom sediments (Caccione and Drake, 1979; Naidu et al., 1984; Eicken et al., 1997).

While the sediment resuspension model used here relies solely on wind-driven and wave-induced oscillatory currents acting on the sea floor to initiate resuspension, the model predicts the onset of sediment resuspension in Elson Lagoon during the ice-free season reasonably well. Good agreement between the potential for resuspension and the AVHRR-derived estimate of turbidity (Figure 5) indicates that sediment resuspension in Elson Lagoon occurs in response to surface gravity waves generated by a particular set of environmental conditions. The primary environmental input parameters of the model are local water depth, fetch and 24-hour resultant wind velocity, suggesting that these parameters are the most critical in determining the onset of sediment resuspension in the lagoon. Therefore, the timing and duration of intense storms that generate surface gravity waves capable of inducing significant sediment resuspension through interactions with bottom sediments in Elson Lagoon are critical in determining water-column sediment concentrations.

The role of tidal and mean ocean currents in the resuspension of bottom sediments along the Arctic nearshore is highly variable. Limited data from the Kara, Laptev and East Siberian Seas indicate that the maximum potential velocity of tidal currents decreases eastward from 20-30 cm/s in the Kara Sea to a few cm/s in the East Siberian

Sea (Pavlov et al., 1996; Kowalik and Proshutinsky, 1994). Tidal current velocities also appear to be small (<10 cm/s) along the Beaufort Sea shelf (T. Weingartner, pers. comm.; Kowalik and Proshutinsky, 1994). Average tidal currents are likely to be significantly smaller, since maximum velocities are often confined to very limited regions, such as near the New Siberian Islands or in narrow passages (cf. Kowalik and Proshutinsky, 1994). Surface mean ocean currents follow a similar geographic trend, decreasing from <20 cm/s in the Kara Sea to <5 cm/s in the East Siberian and Beaufort Seas (T. Weingartner, pers. comm.; Pavlov et al., 1996). Tidal and mean ocean current velocities in the Kara Sea are similar to those found by Cacchione and Drake (1979) and Caccione et al. (1982) in Norton Sound, AK, suggesting that even when tidal current velocities are at a maximum, resuspension is limited unless wind-driven oscillatory waves are also present. Data from Prudhoe Bay, AK on the central Beaufort Sea coast also suggest that tidal current velocities experienced in the East Siberian and western Beaufort Seas (<10 cm/s) are insufficient to resuspend bottom sediment, but could contribute to resuspension in the presence of wave-induced near-bottom oscillatory currents (T. Weingartner, pers. comm.). While wave-induced oscillatory currents are usually necessary to induce bottom sediment resuspension, they may be of sufficient strength for only a portion of the bottom stress necessary for sediment resuspension.

The results of the current study compare favorably to two different theoretical approaches. The first approach (following that of Sharma et al., 1972), estimates the range of grain sizes suspended based on the unidirectional current velocity at the sediment-water interface. The second approach uses a resuspension threshold model

(Komar and Miller, 1973) to estimate whether or not a given grain size is resuspended in the presence of oscillatory water waves. Both approaches predict that fine-grained sediment (mostly silt) would be suspended at all coring locations during the 1998 and 1999 freeze-up periods, but not during the 2000 freeze-up period. A comparison of the models revealed that the resuspension threshold model by Komar and Miller (1973) predicted no resuspension at resuspension potentials (calculated using the model by Booth et al., 2000) less than approximately +4. In Arctic shelf locations where tidal and other ocean currents contribute a significant fraction of the bottom shear stress required to suspend sediment (such as the Kara and Laptev Seas), less contribution is required from wind-induced oscillatory currents to exceed the minimum threshold for sediment movement. In such locations, resuspension should occur at resuspension potentials closer to zero and make the model appear more accurate.

The discrepancy in the resuspension potential required to resuspend sediments according to the two models is consistent with the results of the resuspension model assessment, where resuspension becomes evident only at resuspension potentials greater than +5. One possible explanation for the discrepancy in the onset of resuspension is that the model by Booth et al. (2000) is based on an invalid assumption. The model assumes that resuspension occurs as soon as waves interact with the bottom sediments even though the current velocity induced by these waves at the sediment-water interface may be insufficient to resuspend sediment. Instead, it appears that current velocities corresponding to a resuspension potential of ~+5 are required for the resuspension of bottom sediments. Another possible explanation for the discrepancy in the onset of

resuspension is that the use of high-latitude satellite imagery introduces errors into the percent reflectance calculations employed in assessing the resuspension model's applicability. The surface reflectance of water in the visible and near-infrared wavelengths may be enhanced by the low elevation of the sun during the summer at the latitude of Elson Lagoon.

The bottom-sediment resuspension model also appears to qualitatively predict the sea ice sediment load following fall freeze-up (Tables 2 and 3). In order for bottom sediment to be resuspended, sufficient shear stress must be applied to bottom sediments to entrain them into the water column where they can interact with frazil ice crystals. Increases in bottom shear stress should result in greater amounts of sediment being entrained into the water column, and more interactions between ice crystals and sediment particles. Thus, an increase in the resuspension potential as predicted by the sediment resuspension model should correspond to an increase in the water-column sediment concentration. The presence of frazil ice crystals in all samples implies that the water column was turbulent enough for suspension freezing to take place in all three years (Figure 8). However, as predicted by the sediment resuspension model, bottom shear stress at the sampling sites was only sufficient to resuspend bottom sediment in 1998 and 1999, with greater shear stress occurring in 1999 than in 1998. Of the three model input parameters, wind velocity and fetch vary from year to year, suggesting that these two parameters are responsible for the interannual differences in the magnitudes of resuspension potential and sediment load.

The bathymetry of Elson Lagoon influences the potential for bottom sediment resuspension and the sediment load during each freeze-up event, as well. Resuspension potential maps for all three freeze-up periods (Figure 6) generally exhibit higher resuspension potentials in the southwest half of the study area than in the northeast half. In addition, the general decrease in sediment load from west to east in the 2000 samples mirrors the decrease in the predicted resuspension potential for the 1999 fall freeze-up event (Table 2). These trends parallel trends in the local water depth of the lagoon. The lagoon is shallower in the southwestern half of the study area and deeper in the northeastern half (Figure 4). Thus, higher resuspension potentials and sediment loads correlate with shallower regions and vice versa. The persistence of these correlations from year to year suggests that bathymetry is the dominant model input parameter in determining the spatial variability of sediment resuspension potential and sediment load. Furthermore, the links between the model input parameters, resuspension potential and sea ice sediment load imply that the meter-scale distribution of sediments in sea ice could be estimated by mapping the resuspension potential over a region at the time of freeze-up.

The temporal variability in spatial characteristics exhibited by sediment inclusions in the ice cover of Elson Lagoon appears to be analogous to the spatial variability observed in the Arctic Ocean. As previously indicated, satellite imagery suggests that the regional sediment content of sea ice is patchy. Given the mobility of sea ice and periodic nature of environmental conditions capable of resuspending bottom sediment, this patchy nature is most likely the result of repeated multi-year sea ice formation and export, with the

formation events occasionally coinciding with local resuspension events. Based on the annual fluctuations in sediment concentration observed in Elson Lagoon, it is argued that individual fall freeze-up events in Elson Lagoon are temporal representations of the spatial variability experienced within much larger, shallow, high-latitude marine environments.

4.2 Spatial characteristics of sediment inclusions

Significant variability was found in the spatial characteristics of sedimentary inclusions at the sub-meter scale (Figure 7). The large ranges exhibited by aggregate number densities, mean aggregate cross-sectional areas and mean nearest-neighbor distances indicate that a large degree of spatial variability existed at the sub-centimeter scale (Table 3). The nearest-neighbor statistic provided further support that the small-scale spatial characteristics were not constant. While the nearest-neighbor statistic exhibited little within-core or between-core variance on an annual basis, mean values for 1999 and 2000 fell in the lower half of the potential range of values for this statistic and indicated that some degree of spatial clustering was present. Given the finite size of the analyzed images, the clustering described by the statistic was occurring over the range of micrometers to centimeters. This size range included the scale of individual ice crystals observed in the study.

Results from the microscopic image analysis lend support to the conclusion that significant spatial variability exists at the sub-meter scale, as well (Table 3). Both the aggregate number densities and mean aggregate widths exhibit three-fold differences between the two years. Moreover, since the microscopic analysis was done manually,

these results should be the most reliable. However, strong similarities in trends between the two years in both the macroscopic and microscopic analyses exist suggests that the two different methods yield similar results. Thus, the automated macroscopic imaging technique appears to be a valid method for analyzing sedimentary inclusions in sea ice as long as the limitations imposed by the relatively low resolution are kept in mind.

A number of factors may be responsible for the sub-meter-scale variability in the spatial distribution of sediments. As with the larger scale spatial variability, local water depth may affect the spatial distribution of sediments at smaller scales. However, it is likely that the size of turbulent eddies determines the minimum scale at which local water depth affects the spatial distribution of sediments. The post-freeze-up movement or deformation of the surface ice layer by wind may also affect the sub-meter spatial distribution. While movement over short distances (a few hundred meters at most) is possible, none of the samples exhibited deformation features in the ice that would indicate exposure to strong winds that resulted in long-distance transport after freeze-up.

The nonuniform distribution of sedimentary inclusions in frazil ice may also be due to its association with frazil ice crystals. Previous studies have documented the tendency for frazil ice crystals to capture sedimentary particles as the ice crystals rise through the water column, although the exact mechanism by which the sediment is captured is unknown. The number of captured sedimentary particles appears to be determined by the number of ice crystal-sediment particle interactions. Moreover, the maximum mass (and number, if a relatively constant size is assumed) of adhered sedimentary particles per ice crystal is determined by the buoyancy and surface area of a given crystal, as previously

noted. It has also been documented that individual frazil ice crystals tend to flocculate and this may enhance the filtering of sedimentary particles from the water column during frazil ice formation. These processes appear to control the initial small-scale distribution of sedimentary particles on the surfaces of frazil ice crystals.

Once the frazil ice rises to the ocean surface and begins to solidify, ice growth in the interstices of the slushy layer has been hypothesized to confine sediments in remaining brine inclusions. The fact that sedimentary particles were only observed in brine inclusions (primarily triple junctions and brine pockets) and not within ice crystals in this study supports this hypothesis (Figures 7c and 7d). Also, the large size of frazil crystals compared to the mean aggregate cross-sectional areas, in concert with the relatively small nearest-neighbor statistic values, imply that the tendency toward clustered spatial distributions is a result of the presence of frazil ice crystals in the ice cover. It is likely that the tendency of frazil ice crystals to exclude sediment from the ice crystal structure is responsible for the non-uniform spatial distribution of sediment. As the floating layer of frazil ice begins to solidify, the crystals grow larger and decrease the volume of the brine layer between neighboring ice crystals. Sediment residing in the brine layer is most likely displaced by the advancing crystal faces and physically aggregated into remaining pockets in the brine layer, namely triple junctions and brine pockets.

The overall effect of processes operating during sediment entrainment and sea ice evolution is evident from characteristics of the spatial distribution of sedimentary inclusions. Strong correlations exist between gravimetric sediment concentration, nearest-neighbor distance and mean aggregate cross-sectional area (Figure 11). As

sediment concentration increases, aggregates grow larger (most likely by physical aggregation or flocculation) and the minimum distance between aggregates decreases. The high degree of correlation between these parameters indicates that both mean cross-sectional area and mean nearest-neighbor distance could be estimated from known sediment concentrations. On the other hand, the poor correlation between aggregate number density and sediment concentration implies that neither aggregate number density nor mean inter-aggregate distance can be accurately predicted from conventional measurements of sea ice sediment concentration (Figure 10). Nevertheless, with 61% of the variance in sediment concentration within the frazil layer of first-year sea ice explained by the combination of aggregate number density and aggregate cross-sectional area, it is possible to estimate the combination of these two parameters from measurements of sediment concentration (Figure 12). The persistence of these correlations from year to year indicates that they are independent of space and time. Therefore, one should be able to reconstruct a first-order approximation of the spatial distribution of sedimentary aggregates within the frazil-ice layer of first-year sea ice from sediment concentration.

The values obtained for the volume-to-mass conversion factor and constant "C" in the geometric model imply that much of the entrained sediment occurs as relatively large aggregates that are resolvable with the macroscopic setup. The theoretical value (assuming 0% porosity) for the volume-to-mass conversion factor (2.9×10^6 mg/l) is of the same order of magnitude as the empirical value (2.8×10^6 mg/l). In addition, the value of the unresolvable sediment concentration, "C", (260 mg/l) is relatively small in

comparison to many of the sediment concentrations observed in this study. Thus, the macroscopic approach appears to detect the bulk of entrained sediments, particularly at higher sediment concentrations.

The spatial and temporal variability of sedimentary inclusions in sea ice suggest that there may be similar variability in the amount of nutrients and particle-reactive pollutants present in the ice cover and ultimately delivered to the central Arctic Basin and Nordic Seas. Several potential sources of nutrients (e.g., river deltas) and pollutants (e.g., radioactive waste dumps) are in close proximity to regions likely to contribute large amounts of sediment-associated chemicals to the sea ice cover. Given the reactivity between clay minerals and radioactive contaminants and organic matter, it is likely that sea ice formed during times of greater sediment resuspension could contain higher levels of radioactive contaminants and organic matter than ice formed under relatively calm conditions. Higher concentrations of organic matter may support a greater abundance of bacteria. Increased microbial respiration could enhance biogeochemical changes occurring in the ice cover. Thus, environmental conditions during fall freeze-up are likely to affect the chemical properties of the sea ice cover.

4.3 Environmental conditions and the spatial distribution of sediments

The qualitative agreement between resuspension potential and the large-scale sea ice sediment load found in this study indicates that environmental conditions (i.e., water depth, fetch and wind velocity) during fall freeze-up events play an important role in supplying sediment for entrainment into sea ice. In addition, significant correlations exist between large-scale sea ice sediment concentrations and the small-scale spatial

characteristics of sediment inclusions in sea ice. These correlations suggest that factors controlling the large-scale sediment concentration are also important in determining the small-scale spatial characteristics of the aggregates. Furthermore, this and previous studies (e.g., Weeks and Ackley, 1986; Reimnitz and Kempema, 1987) have shown that the sea ice growth mode is also dependent on environmental conditions during freeze-up. The type of sea ice affects the small-scale spatial distribution of sediment inclusions. Therefore, it appears that environmental conditions influence the small-scale spatial distribution of sediment inclusions by determining the amount of suspended sediment available for entrainment and the type of sea ice present during fall freeze-up events, as depicted in Figure 3. Furthermore, variations in environmental conditions over time appear to cause both temporal and large-scale spatial variability in the distribution of sediments in the sea ice cover.

4.4 Elson Lagoon as a natural laboratory

A number of similarities in the environment between Elson Lagoon and the open shallow shelf suggest that the lagoon is a potential natural laboratory and analog for understanding sea ice sediment properties and sediment entrainment processes in the shelf region. First, periodic storm waves in both of the regions are likely to be the predominant mechanism responsible for resuspending bottom sediments during fall freeze-up both in Elson Lagoon and shallow (<20 m) shelf regions around the Arctic Ocean. Tidal and permanent ocean current velocities are generally small along the Beaufort Sea and East Siberian Sea coasts, but increase toward the Kara Sea. Thus, the entrainment of bottom sediments into the ice cover over the shallow shelves of the

Beaufort and East Siberian Seas should be limited to episodic periods when storm-wave induced sediment resuspension coincides with sea ice formation, as is the case in Elson Lagoon. On the other hand, in the Laptev and Kara Seas the timing of tides may be of additional importance. Second, sediments tend to be fine-grained in both Elson Lagoon and on the Arctic shelves. However, in environments where high tidal and/or ocean current velocities have resulted in the removal of the fine-grained sediment fraction, the lack of muddy sediments would preclude sediment entrainment during suspension freezing, as well. Third, similarities exist in the properties of sea ice found in Elson Lagoon and shallow shelf regions (Nürnberg et al., 1994; Eicken et al., 2000b). The sediment loads documented in this study fall within the range reported by Nürnberg et al. (1994) for the Eurasian shelf and perhaps for Arctic sea ice in general. Also, Eicken et al. (2000b) noted that the properties of sea ice (e.g., temperature and salinity profiles) that forms in Elson Lagoon are comparable to those of both coastal fast ice and drifting ice found in the neighboring Chukchi Sea. These similarities lead one to assume that the processes controlling sediment entrainment and sea ice growth and evolution in some regions of the Arctic Ocean are similar to the processes acting in Elson Lagoon. It seems reasonable then to assume that the processes controlling the spatial distribution of sedimentary particles in the ice should also be similar between Elson Lagoon and the open shallow shelf. Thus, studies of sea ice sediment concentrations and associated spatial characteristics in the lagoon are a potential surrogate for more expensive and logistically challenging transoceanic cruises to study similar characteristics.

There are, however, several differences between Elson Lagoon and the shallow shelf regions in the Arctic that could potentially affect the applicability of the model to these regions. First, the shelf regions are much larger in areal extent and are considerably deeper. While the depth should not pose a problem, the large areal extent would require changes in input data to account for spatial variability in wind velocity. However, these changes should not be difficult to implement in the resuspension model. Second, the hydrography of Elson Lagoon differs from that of the shallow shelf regions in that the latter often exhibit a strong near-surface density stratification due to river runoff (Sherwood, 2000). Sherwood (2000) suggested that this density stratification prevents wind-induced and wave-generated oscillatory currents from reaching the sea floor and would need to be removed by a period of strong winds before sediment could be resuspended. The presence of a density stratification would delay the onset of resuspension, reduce the length of time sediment is resuspended and potentially limit the amount of suspended sediment. Third, there may be a difference between the two environments in the cohesiveness and degree of consolidation of bottom sediments. While the resuspension model assumes that the bottom sediments are poorly cohesive and unconsolidated (as is the case in Elson Lagoon), there is evidence that strongly cohesive and highly consolidated sediments commonly occur on the Arctic shelves (A.S. Naidu, pers. comm.). The presence of cohesive sediments could impair the functionality of the resuspension model in some regions. These differences imply that caution must be exercised when applying the resuspension model to other areas of the Arctic Ocean.

4.5 Potential sources of error in the optical analyses

Several factors may have influenced the results of the micro- and macroscopic image analyses. First, it should be noted that the method employed to determine nearest-neighbor distances ignores the dimensions of the aggregates. Therefore, these measurements represent the distance between the outer surfaces of adjacent particles, rather than between the centers of aggregates. This represents an average error of 12% (assuming spherical aggregates), which is relatively small and should not significantly affect the findings of this study.

Second, the minimum resolution of the macroscopic imaging system (0.026 mm, silt size) may have resulted in the underestimation of aggregate number densities and overestimation of mean aggregate cross-sectional areas and mean nearest-neighbor distances. However, as these are inherent problems in the digital image analysis of objects whose size varies over several orders of magnitude above and below the minimum resolution, it is more important to assess the degree to which this approach biased the data. The geometric model predicts that, on average, 260 mg/l of entrained sediment occurs as unresolvable clasts and aggregates in macroscopic images. This value is relatively low compared to the sediment concentrations exhibited by the bulk of the samples and indicates that the majority of the sediment inclusions are resolved. Thus, the error associated with the minimum resolution is likely to be small, except possibly at low sediment concentrations.

Third, the fact that images of a finite size were analyzed introduces a boundary effect, resulting in the underestimation of nearest-neighbor distances. However, given the

natural variability observed in the samples this error is not deemed important in contrast to other sources of error inherent in our approach.

Fourth, the effect of representing volumes (thin sections) as planar surfaces (images) could potentially result in the overestimation of aggregate number densities and underestimation of nearest-neighbor distances, especially at higher aggregate number densities. A comparison of mean nearest-neighbor distances with sample thickness reveals that, with the exception of core 0005-1, the former are typically of similar magnitude to or larger than the latter. Moreover, even with its greater sample thicknesses, core 0005-1 exhibits mean nearest-neighbor distances that are comparable to core 0005-2, which has similar sediment concentrations. Therefore, representing volumes as planar surfaces does not appear to significantly influence the results of this study.

Finally, the analysis of only vertical thin sections from widely spaced cores may have resulted in an inadequate sampling of the horizontal variability at the centimeter scale. Given the high degree of spatial and temporal variability observed in the samples, it is likely that sampling more frequently spatially would have yielded a more complete picture of the variability exhibited by sea ice sedimentary inclusions. Nevertheless, the reproduction of trends in the macroscopic results by the microscopic analysis together with strong correlations between several parameters imply that the above factors did not significantly bias the results of the macroscopic image analysis.

4.6 Need for future research

While the sediment resuspension model appears suitable for Elson Lagoon, further study is needed to test its applicability to the shallow shelves of the Arctic Ocean. Specifically, the sensitivity of the model to variations in the areal extent and depth of shallow environments must be determined. Also, the impact of variations in the cohesiveness of sediments and of tidal and ocean currents on model results needs to be assessed.

More research also needs to be done on the impact of wave action and the migration of a freeze front on the spatial distribution of sediments. Both wave action and freeze front migration may result in the downward migration and loss of sediments from the slushy layer prior to the solidification of this layer. The potential for the entrainment of sediments into the ice cover by anchor ice also needs to be researched further. Any of these three mechanisms could be responsible for some of the unexplained variability in the spatial distribution of sediments.

In light of predicted changes to the Arctic environment in response to global warming, it is likely that the variability in properties and processes typical of the Arctic sea ice environment may exceed the presently observed range and impact the environment (Serreze et al., 2000). Increased rates of coastal degradation due to thermoerosion of coastal permafrost could result in more sediment being delivered to shallow shelves, the source area of sediments entrained into sea ice. More intense and/or more frequent fall storms around the margins of the Arctic Ocean may entrain greater amounts of sediment into sea ice. Higher sediment concentrations in the ice would

decrease the transmission of light through the ice cover, reducing primary productivity and enhancing summer melt. Enhanced summer melt could lead to more open water and greater fetch around fall freeze-up, resulting in the incorporation of greater sediment loads into sea ice. By comparing future assessments of variability of the Arctic sea ice environment with the natural range of variability predicted by modeling, anthropogenic sources of variability could potentially be elucidated.

Chapter 5

Conclusions

This study demonstrates linkages between environmental conditions and sediment entrainment into sea ice. A simple sediment resuspension model is capable of predicting the onset of sediment resuspension in Elson Lagoon based on a limited number of environmental parameters, namely water depth, wind velocity and fetch. Thus, these three parameters are the dominant variables affecting sediment resuspension in the lagoon. The resuspension model also qualitatively predicts the spatial distribution of sediment loads in the ice cover for a particular year, based on the values of the above parameters from the previous fall freeze-up period.

This study also illustrates connections between sea ice sediment concentrations and the spatial distribution of sedimentary inclusions. Sediment concentration is positively correlated with mean aggregate cross-sectional area, suggesting that physical or chemical aggregation occurs within the ice cover. Sediment concentration is negatively correlated with mean nearest-neighbor distance. Moreover, a geometric model based on mean aggregate cross-sectional area and mean aggregate number density explains 61% of the variance in the sediment concentration of sea ice formed by suspension freezing. The sedimentary inclusions exhibit a somewhat clustered spatial distribution within the ice due to their confinement to intergranular brine inclusions.

Together, the findings of this study imply that environmental conditions at the time of fall freeze-up not only influence the sediment load of sea ice, but also the spatial distribution of sedimentary inclusions in the ice cover. Therefore, the freeze-up

environment may affect the natural variability of the properties of and processes acting in the sea ice environment that are dependent on the presence of sediments (Figure 3). By modeling the freeze-up environment over the full range of naturally occurring conditions, it should be possible to estimate the range of natural variability exhibited by these properties and processes.

References

Aagaard, K., Swift, J.H., Carmack, E.C., 1985. Thermohaline Circulation in the Arctic Mediterranean Seas. Journal of Geophysical Research 90, 4833-3836.

Are, F.E., 1998. The contribution of shore thermoabrasion to the Laptev Sea sediment balance. In: Lewkowicz, A.G., Allard, M (Eds.), Proceedings 7th International Conference on Permafrost, Yellowknife. Université Laval, Centre d'études nordiques, Sainte-Foy, Québec, pp. 25-30.

Barnes, P.W., Reimnitz, E., 1974. Sedimentary processes on arctic shelves off the northern coast of Alaska. In: Reed, J.C., Sater, J.E. (Eds.), The coast and shelf of the Beaufort Sea. Arctic Institute of North America, Arlington, pp. 439-476.

Barnes, P.W., Reimnitz, E., Fox, D., 1982. Ice rafting of fine-grained sediment, a sorting and transport mechanism, Beaufort Sea, Alaska. Journal of Sedimentary Petrology 52, 493-502.

Bischof, J.F., Darby, D.A., 1997. Mid- to Late Pleistocene ice drift in the western Arctic Ocean: evidence for a different circulation in the past. Science 277, 74-78.

Booth, J.G., Miller, R.L., McKee, B.A., Leathers, R.A., 2000. Wind-induced bottom sediment resuspension in a microtidal coastal environment. Continental Shelf Research 20, 785-806.

Caccione, D.A., Drake, D.E., 1979. A new instrument system to investigate sediment dynamics on continental shelves. Marine Geology 30, 299-312.

Caccione, D.A., Drake, D.E., Wiberg. P., 1982. Velocity and bottom-stress measurements in the bottom boundary layer, outer Norton Sound, AK. In: Nelson, C.H., Nio, S. D. (Eds.), The northeastern Bering shelf: new perspectives of epicontinental shelf processes and depositional products. Geologie en Mijnbouw 61, 71-78.

Campbell, N.J., Collin, A.E., 1958. The discoloration of Foxe Basin ice. Journal of the Fisheries Resources Board of Canada 15, 1175-1188.

Clark, D.L, 1990. Arctic Ocean ice cover; geologic history and climatic significance. In: Grantz, A., Johnson, L., Sweeney, J.F. (Eds.), The Arctic Ocean Region. The Geology of North America, vol. L, Geological Society of America, Boulder, pp. 53-62.

Clayton, J.R., Reimnitz, E., Payne, J.R., Kempema, E.W., 1990. Effects of advancing freeze fronts on distributions of fine-grained sediment particles in seawater- and freshwater-slush ice slurries. Journal of Sedimentary Petrology 60, 145-151.

Darby, D.A., Burkle, L.H., Clark, D.L., 1974. Airborne dust on the Arctic pack ice, its composition and fallout rate. Earth and Planetary Science Letters 24, 166-172.

Dethleff, D., Loewe, P., Weiel, D., Nies, H., Kuhlmann, G., Bahe, C., Tarasov, G., 1998. Winter expedition to the southwestern Kara Sea - Investigations on formation and transport of turbid sea ice. Berichte zur Polarforschung 271, 1-40.

Di, L., Rundquist, D.C., 1994. A one-step algorithm for correction and calibration of AVHRR Level 1b data. Photogrammetric Engineering & Remote Sensing 60, 165-171.

Eicken, H., Lange, M.A., 1991. Image analysis of sea-ice thin sections: a step towards automated texture classification. Annals of Glaciology 15, 204-209.

Eicken, H., Reimnitz, E., Alexandrov, V., Martin, T., Kassens, H., Viehoff, T., 1997. Sea-ice processes in the Laptev Sea and their importance for sediment export. Continental Shelf Research 17, 205-233.

Eicken, H., Bock, C., Wittig, R., Miller, H., Poertner, H.-O., 2000b. Magnetic resonance imaging of sea-ice pore fluids: methods and thermal evolution of pore microstructure. Cold Regions Science and Technology 31, 207-225.

Eicken H., Kolatschek, J., Freitag, J., Lindemann, F., Kassens, H., Dmitrenko, I., 2000a. A key source area and constraints on entrainment for basin-scale sediment transport by Arctic sea ice. Geophysical Research Letters 27, 1919-1922.

Hedges, J.I, Keil, R.G., 1995. Sedimentary organic matter preservation: an assessment and speculative synthesis. Marine Chemistry 49, 81-115.

Henley, W.J., Dunton, K.H., 1997. Effects of nitrogen supply and continuous darkness on growth and photosynthesis of the arctic kelp *Laminaria solidungula*. Limnology and Oceanography 42, 209-216.

Hill, P.R., Blasco, S.M., Harper, J.R., Fissel, D.B., 1991. Sedimentation on the Canadian Beaufort Shelf. Continental Shelf Research 11, 821-842.

Horner, R., Schrader, G.C., 1985. Relative contributions of ice algae, phytoplankton, and benthic microalgae to primary production in nearshore regions of the Beaufort Sea. Arctic 35, 485-503.

Intergovernmental Panel on Climate Change (IPCC), 1990. Climate Change: The IPCC Scientific Assessment. Cambridge University Press, p. 365.

Junge, K., Krembs, C., Deming, J., Stierle, A., Eicken, H., 2001. A microscopic approach to investigate bacteria under in-situ conditions in sea ice samples. Annals of Glaciology 33 (in press).

Kempema, E.W., Reimnitz, E., Barnes, P.W., 1989. Sea ice sediment entrainment and rafting in the Arctic. Journal of Sedimentary Petrology 59, 308-317.

Komar, P.D., Miller, M. C., 1973. The threshold of sediment movement under oscillatory water waves. Journal of Sedimentary Petrology 43, 1101-1110.

Kowalik, Z., Proshutinsky, A. Y., 1994. The Arctic Ocean tides. In: Johannessen, O.M., Muench, R.D., Overland, J.E. (Eds.), The polar oceans and their role in shaping the global environment. Geophysical Monograph 85. American Geophysical Union: Washington D. C. pp. 137-158.

Ledley, T.S., Pfirman, S., 1997. The impact of sediment-laden snow and sea ice in the arctic on climate. Climatic Change 37, 641-664.

Light, B., Eicken, H., Maykut, G.A., Grenfell, T.C., 1998. The effect of included particulates on the spectral albedo of sea ice. Journal of Geophysical Research 103, 27739-27752.

Macdonald, R.W., Solomon, S.M., Cranston, R.E., Welch, H.E., Yunker, M.B., Gobeil, C., 1998. A sediment and organic carbon budget for the Canadian Beaufort Shelf. Marine Geology 144, 255-273.

Maykut, G.A., 1986. The surface heat and mass balance. In: Untersteiner, N. (Ed.), The geophysics of sea ice. Martinus Nijhoff Publ., Dordrecht (NATO ASI B146), pp. 395-463.

Measures, C.I., 1999. The role of entrained sediments in sea ice in the distrbution of aluminium and iron in the surface waters of the Arctic Ocean. Marine Chemistry 68, 59-70.

Naidu, A.S., Cooper, L.W., 1998. Clay mineral composition of ice-rafted sediments collected from the 1994 Arctic Ocean Section, eastcentral Chukchi Sea-North Pole. Proceedings of the American Geophysical Union Fall Meeting, San Francisco.

Naidu, A.S., Larsen, L.H., Sweeney, M.D., Weiss, H.V., 1980. Sources, transport pathways, depositional sites and dynamics of sediments in the lagoon and adjacent shallow marine region, northern Arctic Alaska. U.S. Department of Commerce, National Oceanic and Atmospheric Administration, Outer Continental Shelf Environmental Assessment Program (OCSEAP) Annual Report 7, 3-93.

Naidu, A.S., Larsen, L.H., Mowatt, T.C., Sweeney, M.D., Weiss, H.V., 1982. Aspects of size distributions, clay mineralogy and geochemistry of sediments of the Beaufort Sea and adjacent deltas, north Arctic Alaska. U.S. Department of Commerce, National Oceanic and Atmospheric Administration, Outer Continental Shelf Environmental Assessment Program (OCSEAP) Annual Report 33, 315-429.

Naidu, A.S., Mowatt, T.C., Rawlinson, S.E., Weiss, H.V., 1984. Sediment characteristics of the lagoons of the Alaskan Beaufort Sea coast, and evolution of Simpson Lagoon. In: Barnes, P.W., Schell, D.M., Reimnitz, E. (Eds.), The Alaskan Beaufort Sea. Ecosystems and Environments. Academmic Press, London, pp. 275-292.

Naidu, A.S., Cooper, L.W., Finney, B.P., Macdonald, R.W., Alexander, C., Semiletov, I.P., 2000. Organic carbon isotope ratios ($\delta^{13}C$) of Arctic Amerasian continental shelf sediments. International Journal of Earth Sciences 89, 522-532.

Nies, H., Harms, I.H., Karcher, M.J., Dethleff, D., Bahe, C., 1999. Anthropogenic radioactivity in the Arctic Ocean - review of the results from the joint German project. The Science of the Total Environment 237/238, 181-191.

Nummedal, D, 1979. Coarse-grained sediment dynamics - Beaufort Sea, Alaska. In: Proceedings 5th Conference on Port and Ocean Engineering under Arctic Conditions, Trondheim, vol. II, pp. 845-858.

Nürnberg, D., Wollenburg, I., Dethleff, D., Eicken, H., Kassens, H., Letzig, T., Reimnitz, E., Thiede, J., 1994. Sediments in Arctic sea ice: implications for entrainment, transport and release. Marine Geology 119, 185-214.

Osterkamp, T.E., Gosink, J.P., 1984. Observations and analyses of sediment-laden sea ice. In: Barnes, P.W., Schell, D.M., Reimnitz, E. (Eds.), The Alaskan Beaufort Sea. Ecosystems and Environments. Academmic Press, London, pp. 73-93.

Pavlov, V.K., Timokhov, L.A., Baskakov, G.A., Kulakov, M.Y., Kurazhov, V.K., Pavlov, P.V., Pivovarov, S.V., Stanovoy, V.V., 1996. Hydrometeorological Regime of the Kara, Laptev, and East-Siberian Seas, Technical Memorandum APL-UW TM 1-96. Applied Physics Laboratory, University of Washington, Seattle, p. 179.

Perovich, D.K., Gow, A.J., 1996. A quantitative description of sea ice inclusions. Journal of Geophysical Research 101, 18327-18343.

Pfirman, S., Colony, R., Nürnberg, D., Eicken, H., Rigor, I., 1997. Reconstructing the origin and trajectory of drifting arctic sea ice. Journal of Geophysical Research 102, 12575-12586.

Pond, S., Pickard, G.L., 1983. Introductory Dynamical Oceanography. Butterworth-Heinemann: Boston, p. 329.

Rasband W.S., Bright, D.S., 1995. NIH Image: a public domain image processing program for the Macintosh. Journal of Microbeam Analysis 4, 137-149.

Reimnitz, E., Kempema, E.W., 1987. Field observations of slush ice generated during freeze-up in Arctic coastal waters. Marine Geology 77, 219-231.

Reimnitz, E., Kempema, E.W., Barnes, P.W., 1987. Anchor ice, seabed freezing and sediment dynamics in shallow arctic seas. Journal of Geophysical Research 92, 14671-14678.

Reimnitz, E., Dethleff, D., Nürnberg, D., 1994. Contrasts in Arctic shelf sea-ice regimes and some implications: Beaufort Sea versus Laptev Sea. Marine Geology 119, 215-225.

Reimnitz, E., McCormick, M., McDougall, K., Brouwers, E., 1993. Sediment export by ice rafting from a coastal polynya, Arctic Alaska, USA. Arctic and Alpine Research 25, 83-98.

Reimnitz, E., McCormick, M., Bischof, J., Darby, D.A., 1998. Comparing sea-ice sediment load with Beaufort Sea shelf deposits: Is entrainment selective? Journal of Sedimentary Research 68, 777-787.

Serreze, M.C., Walsh, J.E., Chapin III, F.S., Osterkamp, T., Dyurgerov, M., Romanovsky, V., Oechel, W.C., Morison, J., Zhang, T., Barry, R.G., 2000. Observational evidence of recent change in the northern high-latitude environment. Climatic Change 46, 159-207.

Sharma, G.D., Naidu, A.S., Hood, D.W., 1972. Bristol Bay: model contemporary graded shelf. American Association of Petroleum Geologists Bulletin 56, 2000-2012.

Sherwood, C.R., 2000. Numerical model of frazil ice and suspended sediment concentrations and formation of sediment laden ice in the Kara Sea. Journal of Geophysical Research 105, 14061-14080.

Swan, A.R.H., Sandilands, M., 1995. Introduction to Geological Data Analysis. Blackwell Science: Malden, MA, p. 446.

Tynan, C.T., DeMaster, D.P., 1997. Observations and predictions of Arctic climate change: potential effects on marine mammals. Arctic 50, 308-322.

U.S. Army Coastal Engineering Research Center (CERC), 1984. Shore protection manual. Vol. 1: 4th Edition. U.S. Army Coastal Engineering Center; Fort Belvoir, VA, p. 603.

Weeks, W.F., Ackley, S.F., 1986. The growth, structure and properties of sea ice. In: Untersteiner, N. (Ed.), The geophysics of sea ice. Martinus Nijhoff Publ., Dordrecht (NATO ASI B146), pp. 9-164.

Wiseman, Jr., W.J., Coleman, J.M., Gregory, A., Hsu, S.A., Short, A.D., Suhayda, J.N., Walters, Jr., C.D., Wright., L.D., 1973. Alaskan arctic coastal processes and morphology. Louisiana State University, Coastal Studies Institute Technical Report 149. Coastal Studies Institute, Baton Rouge, p. 171.

Zatsepin, A.G., Golovin, P.N., 2001. Laboratory experiments on frazil ice formation with application to the arctic marine environment. Memoirs of National Institute of Polar Research, Special Issue 54, 417-421.